



## Physical controls on CH<sub>4</sub> emissions from a newly flooded subtropical freshwater hydroelectric reservoir: Nam Theun 2

C. Deshmukh<sup>1,2,\*</sup>, D. Serça<sup>1</sup>, C. Delon<sup>1</sup>, R. Tardif<sup>3</sup>, M. Demarty<sup>4</sup>, C. Jarnot<sup>1</sup>, Y. Meyerfeld<sup>1</sup>, V. Chanudet<sup>5</sup>, P. Guédant<sup>3</sup>, W. Rode<sup>3</sup>, S. Descloux<sup>5</sup>, and F. Guérin<sup>6,7</sup>

<sup>1</sup>Laboratoire d'Aérodynamique – Université de Toulouse – CNRS UMR 5560; 14 Av. Edouard Belin, 31400, Toulouse, France

<sup>2</sup>TERI University, New Delhi, India

<sup>3</sup>Nam Theun 2 Power Company Limited (NTPC), Environment & Social Division – Water Quality and Biodiversity Dept. – Gnommalath Office, P.O. Box 5862, Vientiane, Lao PDR

<sup>4</sup>Environnement Illimité, 1453 rue Saint Timothee, Montreal QC, Canada

<sup>5</sup>Electricité de France, Hydro Engineering Centre, Sustainable Development Dpt, Savoie Technolac, 73373, Le Bourget du Lac, France

<sup>6</sup>Université de Toulouse; UPS GET, 14 Avenue E. Belin, 31400, Toulouse, France

<sup>7</sup>IRD; UR 234, GET ; 14 Avenue E. Belin, 31400, Toulouse, France

\* now at: Nam Theun 2 Power Company Limited (NTPC), Environment & Social Division – Water Quality and Biodiversity Dept. – Gnommalath Office, P.O. Box 5862, Vientiane, Lao PDR

Correspondence to: D. Serça (dominique.serca@aero.obs-mip.fr)

Received: 3 February 2014 – Published in Biogeosciences Discuss.: 26 February 2014

Revised: 28 May 2014 – Accepted: 20 June 2014 – Published: 13 August 2014

**Abstract.** In the present study, we measured independently CH<sub>4</sub> ebullition and diffusion in the footprint of an eddy covariance system (EC) measuring CH<sub>4</sub> emissions in the Nam Theun 2 Reservoir, a recently impounded (2008) subtropical hydroelectric reservoir located in the Lao People's Democratic Republic (PDR), Southeast Asia. The EC fluxes were very consistent with the sum of the two terms measured independently (diffusive fluxes + ebullition = EC fluxes), indicating that the EC system picked up both diffusive fluxes and ebullition from the reservoir. We showed a diurnal bimodal pattern of CH<sub>4</sub> emissions anti-correlated with atmospheric pressure. During daytime, a large atmospheric pressure drop triggers CH<sub>4</sub> ebullition (up to 100 mmol m<sup>-2</sup> d<sup>-1</sup>), whereas at night, a more moderate peak of CH<sub>4</sub> emissions was recorded. As a consequence, fluxes during daytime were twice as high as during nighttime.

Additionally, more than 4800 discrete measurements of CH<sub>4</sub> ebullition were performed at a weekly/fortnightly frequency, covering water depths ranging from 0.4 to 16 m and various types of flooded ecosystems. Methane ebullition varies significantly seasonally and depends mostly on water level change during the warm dry season, whereas no rela-

tionship was observed during the cold dry season. On average, ebullition was  $8.5 \pm 10.5$  mmol m<sup>-2</sup> d<sup>-1</sup> and ranged from 0 to 201.7 mmol m<sup>-2</sup> d<sup>-1</sup>.

An artificial neural network (ANN) model could explain up to 46 % of seasonal variability of ebullition by considering total static pressure (the sum of hydrostatic and atmospheric pressure), variations in the total static pressure, and bottom temperature as controlling factors. This model allowed extrapolation of CH<sub>4</sub> ebullition on the reservoir scale and performance of gap filling over four years. Our results clearly showed a very high seasonality: 50 % of the yearly CH<sub>4</sub> ebullition occurs within four months of the warm dry season. Overall, ebullition contributed 60–80 % of total emissions from the surface of the reservoir (disregarding downstream emissions), suggesting that ebullition is a major pathway in young hydroelectric reservoirs in the tropics.

## 1 Introduction

The atmospheric methane (CH<sub>4</sub>) mixing ratio has recently reached up to 1875 ppb, which is 162 % higher than the pre-industrial value (IPCC, 2013), and is the highest mixing ratio ever reported (Dlugokencky et al., 2009). Currently, CH<sub>4</sub> is directly and indirectly responsible for 43 % of the anthropogenic radiative forcing (IPCC, 2013). Emissions from aquatic ecosystems (wetlands and inland freshwaters) are the main source of CH<sub>4</sub> on Earth (IPCC, 2013), representing 40 % of total CH<sub>4</sub> emissions and 75 % of natural CH<sub>4</sub> emissions (IPCC, 2013). Emissions from inland freshwaters alone would correspond to 50 % of the carbon terrestrial sink (Bastviken et al., 2011). The order of magnitude of CH<sub>4</sub> emissions from inland waters is probably conservative (Bastviken et al., 2011). However, these estimates are based on a data set characterized by low temporal and spatial resolution (Bastviken et al., 2004; Barros et al., 2011), although a few studies evidenced strong diurnal variations (Bastviken et al., 2010; Sahlée et al., 2014), seasonal variability (e.g. Abril et al., 2005), transient extreme emissions (e.g. Varadharajan and Hemond, 2012; Sahlée et al., 2014), and strong spatial variations (e.g. Del Sontro et al., 2011; Morrissey and Livingstone, 2012). It is therefore possible that hot moments and hot spots of emissions were overlooked, leading to a potential underestimation of emissions on a global scale.

Among the different known CH<sub>4</sub> pathways to the atmosphere, diffusive fluxes and, to a lesser extent, ebullition have been the most studied ones in natural lakes and anthropogenic water bodies (i.e. hydroelectric reservoirs, farm ponds, etc.). Methane ebullition corresponds to vertical transfer of CH<sub>4</sub> from the sediment to the atmosphere, with little physical and biological interactions within a shallow (< 20m) water column (McGinnis et al., 2006). Methane is produced under anoxic conditions in the sediments or the flooded soils during the mineralization of organic matter. CH<sub>4</sub> bubbles can develop if the CH<sub>4</sub> concentration in the interstitial water becomes higher than the maximum solubility of this gas in water. Bubbling fluxes mainly occur in the shallow parts of lakes and hydroelectric reservoirs (Abril et al., 2005; Bastviken et al., 2004; Galy-Lacaux et al., 1997; Keller and Stallard, 1994), where the hydrostatic pressure is low. The release of the bubbles is triggered by atmospheric pressure variations (Casper et al., 2000; Eugster et al., 2011; Fechner-Levy and Hemond, 1996; Mattson and Likens, 1990; Tokida et al., 2005; Wik et al., 2013), variations in water current velocity (Martens and Klump, 1980; Chanton et al., 1989), shear stress at the sediment surface (Joyce and Jewell, 2003), variation in the water level above the sediment (e.g. Boles et al., 2001; Chanton et al., 1989; Engle and Melack, 2000; Martens and Klump, 1980; Smith et al., 2000), an increase in temperature that makes the CH<sub>4</sub> solubility decrease (Chanton and Martens, 1988), and strong wind events (Keller and Stallard, 1994). Ebullition is episodic, which makes it difficult to quantify accu-

ately. Bubbling fluxes are probably always underestimated (Bastviken et al., 2011; Glaser et al., 2004; Wik et al., 2013); thus, they must be determined as frequently as possible. In most of the ecosystems where it was determined by discrete sampling with funnels or floating chambers, ebullition was shown to dominate diffusive fluxes (Bastviken et al., 2011).

Diffusive CH<sub>4</sub> fluxes at the air–water interface depend on the concentration gradient between the surface water and the atmosphere and the gas transfer velocity (Wanninkhof, 1992). They are usually estimated either by calculations or by floating chambers (FCs). The calculation by the thin boundary layer (TBL) model (Liss and Slater, 1974) is based on the concentration gradient between the water surface and the atmosphere and a gas transfer velocity. In the literature, the gas transfer velocity and thus the diffusive fluxes are related for instance to wind speed (e.g. Borges et al., 2004; Cole et Caraco, 1998; Frost and Upstill-Goddard, 2002; Guérin et al., 2007), rainfall rates (Ho et al., 1997; Guérin et al., 2007), buoyancy fluxes (MacIntyre et al., 2011), or water current velocity (e.g. Borges et al., 2004). The limit of this approach is that these relationships are site specific (Borges et al., 2004; Kremer et al., 2003b), leading to uncertainties when applied without precaution. Fluxes can also be obtained on site by the use of FCs. This technique is frequently criticized because FCs are supposed to either artificially increase turbulence, especially at low wind speed (Matthews et al., 2003; Vachon et al., 2010), or to decrease turbulence by isolating the surface water from the wind friction (Liss and Merlivat, 1986). Nevertheless, FCs were shown to give results in fair agreement compared to other methods in some aquatic ecosystems (Kremer et al., 2003a; Guérin et al., 2007; Cole et al., 2010; Gålfalk et al. 2013). FCs capture both diffusive flux and ebullition if present. In low ebullition conditions, these flux components can be separated by variability patterns among replicate chambers (e.g. Bastviken et al., 2004). In high-ebullition environments, bubble shields may be needed to estimate diffusive flux by excluding ebullition from some chambers (Bastviken et al., 2010).

Eddy covariance (EC) measurements of CH<sub>4</sub> emissions are becoming feasible with suitable fast-response sensors now available on the market (Eugster and Plüss, 2010; McDermitt et al., 2010). It is therefore realistic to quantify CH<sub>4</sub> emissions with EC technique on a scale representative of a wide range of ecosystems. Still, very few EC field deployments have been conducted so far to determine CH<sub>4</sub> emissions, whether in freshwater lakes (Schubert et al., 2012) or man-made reservoirs (e.g. Eugster et al., 2011). EC was shown to be able to capture both diffusive flux and ebullition (Eugster et al., 2011), but with no discrimination between the two pathways. The deployment of EC that captures continuously the emissions with a short time resolution (e.g. 30 min) over long periods (days to years) and large areas (typically hectares), in combination with the intensive deployment of classical discrete sampling methodology for the estimation of diffusion and ebullition, should allow the determination of

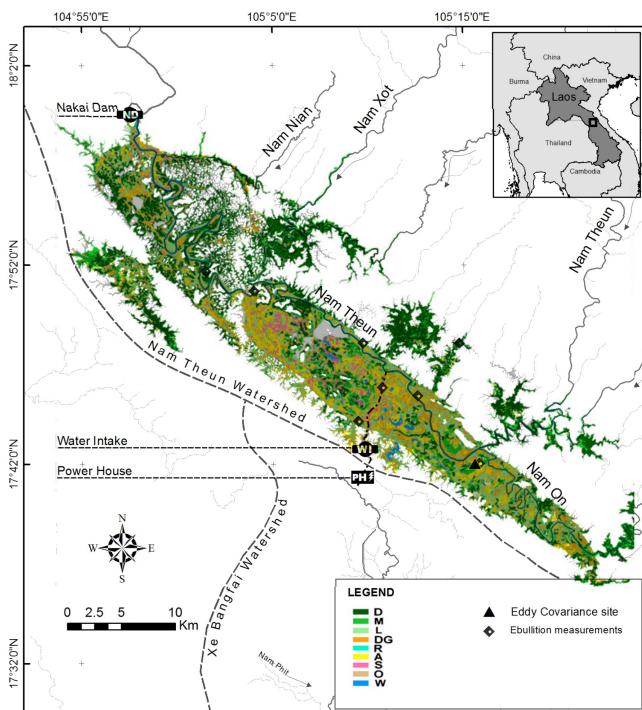


**Figure 1.** Map of the Nam Theun 2 hydroelectric reservoir (Lao People's Democratic Republic) showing (1) the land cover before flooding (from Descloux et al., 2011), with D: dense forest, M: medium forest, L: light forest, DG: degraded forest, R: riparian forest, A: agricultural soils, S: swamps, O: others and W: water, and (2) the location of the ebullition measurements and the eddy covariance site.

the controlling factors on the short-term, daily and seasonal variability of CH<sub>4</sub> emissions by its different pathways.

In the present study, CH<sub>4</sub> emission was measured with EC, FC and funnels, and calculated by TBL at the Nam Theun 2 (NT2) Reservoir in Lao PDR, Southeast Asia. This man-made lake was chosen because of its potential for high CH<sub>4</sub> emissions owing to its recent impoundment (2008) (Abril et al., 2005; Barros et al., 2011), and for the fact that it encompasses large and fast water level variations that should enhance ebullition (e.g. Chanton et al., 1989) compared to most of the natural lakes and wetlands. First, the different methods were compared according to the CH<sub>4</sub> pathways they capture. Once all methods were validated, high-frequency measurements over diurnal cycles at different seasons obtained with EC were used for the determination of the physical controls on CH<sub>4</sub> emissions and pathways on a daily basis. Based on a weekly monitoring of ebullition during one and a half years, we examined its controlling factors in order to estimate ebullition on the entire reservoir scale. This was finally achieved with an artificial neural network approach which allowed us to simulate over a four-year period the ebullition for the entire reservoir from the controlling factors.

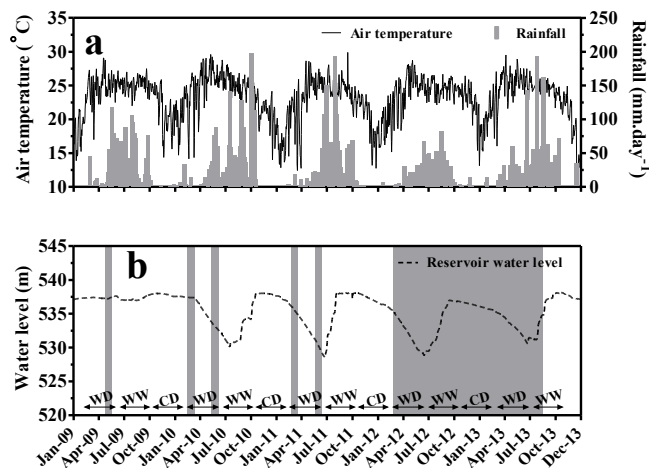


**Figure 2.** Time series of (a) air temperature and rainfall rates and (b) the Nam Theun 2 Reservoir water level during the study. The grey bars and shaded area indicate the field experiments and the ebullition monitoring, respectively. The double arrows indicate the seasons (WD: warm dry; WW: warm wet; CD: cold dry).

## 2 Site description

The Nam Theun 2 (NT2) hydroelectric reservoir (17°59'49" N, 104°57'08" E) was built on the Nam Theun River, in the subtropical region of the Lao PDR. Filling of the reservoir began in April 2008, and the full water level of the reservoir (538 m msl) was reached for the first time in October 2009. At maximal water level, the reservoir floods a 489 km<sup>2</sup> dendritically shaped area which was mainly covered by dense and medium forests (44.7%), light and degraded forests (36.4%), and agricultural lands (11%), with the rest made up of swamps and rivers (Descloux et al., 2011, Fig. 1).

The study site is under a subtropical monsoon climate. The classical meteorological years can be separated into three seasons: a warm wet (WW) season from mid-June to mid-October, a cool dry (CD) season from mid-October to mid-February, and a warm dry (WD) season from mid-February to mid-June (Fig. 2). Since the water inputs to the NT2 Reservoir are directly related to rainfall, filling of the reservoir typically occurs during the WW season, when the study area receives 80% of its annual rainfall (NTPC, 2005). Since the beginning of the power plant operation (March 2010), the reservoir water level has varied seasonally, and achieved its maxima during the WW season and minima by the end of the WD season. During the period covered by this study, the reservoir water level varied seasonally by up to 9.5 m (Fig. 2), which corresponded to a variation in the reservoir water surface of 168 to 489 km<sup>2</sup>. With an annual average depth of 7.8 m, the NT2 Reservoir falls into the shallow reservoir category.

### 3 Methods

#### 3.1 Sampling strategy

The EC system was deployed in an open water area (17°41.56' N, 105°15.36' E) chosen to offer a smooth fetch in all directions. At this location, fetch varied from about 1 km (northeast) to more than 10 km (northwest). Eddy covariance was deployed four times to study the CH<sub>4</sub> emissions under a variety of meteorological and environmental conditions. Two deployments (3 days in May 2009 and 5 days in June 2011) were performed during the transition between the WD season and the WW season (Fig. 2). The average water depth was ~10 and ~1.5 m in May 2009 and June 2011, respectively. The other two field campaigns (14 days in March 2010 and 5 days in March 2011) occurred during the transition between the CD and WD seasons (Fig. 2). Average water depth was ~10.5 m and ~6.5 m in March 2010 and March 2011, respectively. During the May 2009 campaign, the reservoir water level increased at a mean rate of 1.0 cm d<sup>-1</sup>, whereas the other three campaigns were performed during a falling reservoir water level, at mean rates of -4.5, -4.6 and -6.9 cm d<sup>-1</sup>, respectively for March 2010, March 2011 and June 2011 (Fig. 2). Statistical details of the different meteorological parameters for the four EC deployments are summarized in Supplement Table S1.

During each EC deployment, independent measurements of the diffusive and ebullitive fluxes were performed in the footprint of the EC set-up with FC and funnels, respectively. Each FC measurement was taken together with surface water sampling devoted to the determination of the CH<sub>4</sub> concentration. Note that in March 2010, funnel measurements could not have been performed around the EC set-up.

Additional CH<sub>4</sub> ebullition measurements were performed with funnels during five field campaigns covering different seasons, from May 2009 to June 2011, and during weekly monitoring from March 2012 to August 2013. During this monitoring, spatial variation was explored through measurements at 44 locations spread over seven stations (Fig. 1) representative of the different types of flooded ecosystems (dense and medium forests, light and degraded forest and agricultural lands, Descloux et al., 2011), and with different depths (from 0.4 to 16 m) at each sampling site.

#### 3.2 Instrumentation of the EC system

The basic EC instrumentation included a 3-D sonic anemometer (Windmaster Pro, Gill Instruments, Lymington, Hampshire, UK, in May 2009 and March 2010, and a CSAT-3, Campbell Scientific, Logan, UT, USA, in March 2011 and June 2011), and a closed-path fast methane analyser (DLT-100 FMA, Los Gatos Research, CA, USA). Data acquisition was carried out at 10 Hz with a Campbell data logger (CR3000 Micrologger<sup>®</sup>, Campbell Scientific).

Air was carried to the DLT-100 through a 6 m long tube (Synflex-1300 tubing, Eaton Performance Plastics, Cleveland) with an internal diameter of 8 mm. The tube inlet, protected by a plastic funnel to avoid entry of rainwater, was mounted 0.20 m behind the sonic anemometer sensors. An internal 2 µm Swagelok filter was used to protect the sampling cell from dust, aerosols, insects and droplets. High-frequency sampling of air was obtained by the use of a dry vacuum scroll pump (XDS35i, BOC Edwards, Crawly, UK) providing a flow rate of 26 L min<sup>-1</sup>. Due to the remote location of our study site, a 5 kVA generator running on gasoline was used for the power supply of the whole EC instrumentation. Possible contaminations of the atmospheric CH<sub>4</sub> concentration measurements from the generator were checked using the wind direction and a footprint model (Kljun et al., 2004). The footprints during the four deployments are shown in Supplement Fig. S1.

During each EC deployment, wind speed, wind direction, atmospheric pressure, atmospheric temperature, relative humidity and rainfall were measured using a meteorological station (Weather Transmitter Model WXT510, Helsinki, Finland). A radiometer (CNR-1, Kipp & Zonen, Delft, The Netherlands) was used to measure incoming and outgoing shortwave and longwave radiations. The temperature of the surface water was measured at 20 cm depth using a thermistor (Pt100 sensor) coupled to the data logger.

#### 3.2.1 Data processing

The 10 Hz raw data were processed using the EdiRe software (Clement, 1999) for the following steps: (1) spike detection using a standard de-spiking algorithm whereby wind vector and scalar values greater than three times the standard deviation are removed, (2) lag correction and tube attenuation relevant to the closed-path DLT-100 gas analyser, (3) coordinate rotation using the planar fit method, and (4) high-frequency correction factors to take into account the loss at high frequency due to an insufficient sampling rate.

Differences between the deployment-specific variables, i.e. sensor separation distance and instrument placement, were considered while processing the data. The EC fluxes of CH<sub>4</sub> were calculated as the covariance between the scalars and vertical wind speed fluctuations according to commonly accepted procedures (Aubinet et al., 2001). Fluxes were considered positive if they were directed from the water surface toward the atmosphere, and negative otherwise.

#### 3.2.2 EC data quality control

Fluxes were accepted or rejected according to the following criteria. First, a non-stationarity criterion was applied according to Foken and Wichura (1996). Fluxes were considered stationary and therefore accepted only if the difference between the mean covariance of sub-records (5 min) and the covariance of the full period (30 min) was less than 30 %.

Second, a flux was rejected if its intermittency rose above 1 (Mahrt et al., 1998). Third, for a vertical wind component, the skewness and kurtosis were used to stay within the range of  $(-2, 2)$  and  $(1, 8)$ , respectively (Vickers and Mahrt, 1997). Fourth, the momentum flux,  $u'w'$ , was required to be negative, implying a downward directed momentum flux. In addition, fluxes were rejected when the wind came from the power generator unit according to the footprint model of Kljun et al. (2004). For footprint analysis, since the roughness length value was unknown, we considered a value of 0.0002 m, as reported for terrain without obstacle (WMO, 2008). According to the model, the footprint was different in extension and prevalent wind directions among the different field campaigns. The smallest footprint area was observed during the March 2010 campaign, and the biggest for June 2011, with the greatest values rarely exceeding 500 m. The analysis confirmed that (1) surrounding terrestrial ecosystems were always outside the footprint (Supplement Fig. S1), (2) only 2 % of the fluxes were rejected because wind came from the power generator, and (3) all FC and funnels measurements were conducted within the EC footprint area.

As mentioned by Eugster et al. (2011), the minimum threshold for friction velocity cannot apply as a good criterion for flux rejection, since turbulence generated due to heat loss from the water column can contribute significantly to the emissions into the atmosphere (Eugster et al., 2003, 2011; MacIntyre et al., 2002, 2010). In addition, the criteria for atmospheric concentration formulated by Vickers and Mahrt (1997) for CO<sub>2</sub> over terrestrial ecosystems do not apply for CH<sub>4</sub> over an aquatic ecosystem, since emissions could be sporadic due to a potential CH<sub>4</sub> burst linked to ebullition (Eugster et al., 2011).

Quality control criteria applied all together resulted in the acceptance of 57 % of the flux data, with acceptance rates slightly higher during daytime (59 %) than nighttime (52 %) periods.

### 3.3 Diffusive fluxes

#### 3.3.1 Measurement by floating chamber (FC)

Diffusive flux measurements around the EC site were performed with two circular floating chambers (FC<sub>GC</sub>, surface area = 0.15 m<sup>2</sup>; volume = 24.6 L), following the same design as in Guérin et al. (2007). Moreover, FCs were covered with a reflective surface to limit warming inside the chamber during measurements. Duplicate samples were taken from the FCs at time 0 and then every 15 min for 45 min, for a total of four samples per chamber deployment. In the chambers, samples were collected in 10 mL glass vials which contained a 6M NaCl solution capped with butyl stoppers and aluminium seals as described in Angel and Conrad (2009). All samples were analysed within 48 h by gas chromatography (GC). Diffusive fluxes (D<sub>GC</sub>) were calculated from the slope of the

linear regression of gas concentration in the chamber versus time. Diffusion chambers will collect diffusive emissions as well as ebullitive emissions if they are present. Therefore, if the slope of the linear regression of gas concentration in the chamber versus time was linear, with  $r^2 > 0.8$ , then the chamber was assumed to be collecting only diffusive emissions (D<sub>GC</sub>). If  $r^2 < 0.8$ , then the chamber was assumed to collect total (diffusive + ebullitive) emissions (subsequently denoted as DE<sub>GC</sub>; see Sect. 4.1).

In March 2011, a floating chamber (surface area = 0.16 m<sup>2</sup>; volume = 17.6 L) connected to a Picarro<sup>®</sup> CH<sub>4</sub> analyser (FC<sub>GA</sub>) was also deployed to measure diffusive fluxes (D<sub>GA</sub>). The calculation and rejection procedures are identical to the ones described above for D<sub>GC</sub>.

#### 3.3.2 Estimate from surface CH<sub>4</sub> concentrations

Surface water samples for CH<sub>4</sub> concentration were taken with a surface water sampler described by Abril et al. (2007). Water samples were stored in 60 mL glass vials, capped with butyl stoppers, sealed with aluminium crimps, and poisoned until analysis (Guérin and Abril, 2007). Before GC analysis for CH<sub>4</sub> concentration, a N<sub>2</sub> headspace was created and the vials were shaken vigorously to ensure an equilibration between the liquid and gas phases (i.e. Guérin and Abril, 2007). The specific gas solubility for CH<sub>4</sub> (Yamamoto et al., 1976) as a function of temperature was used for the calculation of CH<sub>4</sub> concentrations dissolved in water.

The surface CH<sub>4</sub> concentrations were used together with atmospheric concentrations measured on site in order to calculate diffusive fluxes with Eq. (1):

$$D_{\text{TBL}} = k_T \times C_w - C_a, \quad (1)$$

where  $D_{\text{TBL}}$  is the diffusive flux at the water–air interface,  $k_T$  the gas transfer velocity for a given temperature ( $T$ ),  $C_w$  the CH<sub>4</sub> concentration in surface water, and  $C_a$  the CH<sub>4</sub> concentration in the surface water at equilibrium with the overlying atmosphere. The  $k_T$  values were computed with the following Eq. (2):

$$k_T = k_{600} \times (600/Sc_T)^n, \quad (2)$$

with  $k_{600}$  the gas transfer velocity of CO<sub>2</sub> at 20 °C,  $Sc_T$  the Schmidt number of CH<sub>4</sub> at a given temperature ( $T$ ) (Wanninkhof, 1992), and  $n$  a number that is either 2/3 for low wind speed ( $< 3.7 \text{ m s}^{-1}$ ) or 0.5 for higher wind speed (Jähne et al., 1987). The  $D_{\text{TBL}}$  values were calculated according to the formulation of  $k_{600}$  versus wind speed from MacIntyre et al. (2010) and Guérin et al. (2007), the average of both formulations being used in the manuscript. These formulations were chosen because MacIntyre et al. (2010) includes the effect of buoyancy fluxes in the gas transfer velocity, and because Guérin et al. (2007) is one of the very few available for tropical hydroelectric reservoirs.

### 3.4 CH<sub>4</sub> ebullition

Clusters of five to ten PET funnels (diameter = 26 cm, height = 30 cm) attached to each other at 1 m distance were assembled. Three to six clusters were positioned below the water surface at locations with different water depths around the same site (within 10–30 m). The funnels remained on site for 24 or 48 h. Accumulated gas volumes during the deployment period were collected manually through a butyl-rubber septum using a 60 mL syringe at the end of the experiment, as described in Wik et al. (2013). The gas sample was stored in glass vials which contained a 6 M NaCl solution. All gas samples were analysed for CH<sub>4</sub> within 48 h by GC. CH<sub>4</sub> concentration in bubbles was multiplied by the volume of accumulated gas ( $V_{EB}$ , mL m<sup>-2</sup> d<sup>-1</sup>) over the deployment period to determine CH<sub>4</sub> ebullition fluxes ( $E_{FUN}$ ).

The ebullition was also determined from the FC<sub>GA</sub> measurements in March 2011. The sudden increase in the CH<sub>4</sub> concentrations in the FC<sub>GA</sub> was attributed to bubbles. Methane ebullition ( $E_{GA}$ ) was calculated from the increase in CH<sub>4</sub> concentrations in the chamber, the deployment time of FC<sub>GA</sub> measurement (typically 5–20 min), and the surface of the chamber.

### 3.5 Gas chromatography

Analysis of CH<sub>4</sub> concentration was performed by gas chromatography (SRI<sup>®</sup> 8610C gas chromatograph, Torrance, CA, USA) equipped with a flame ionization detector (FID). A subsample of 0.5 mL from the headspace of water sample vials and 1 mL of air from flux sample vials were injected. Commercial gas standards (2, 10 and 100 ppmv, Air Liquide “crystal” standards and a mixture of N<sub>2</sub> with 100 % CH<sub>4</sub>) were injected after an analysis of every 10 samples for calibration. Duplicate injection of samples showed a repeatability better than 5 %.

### 3.6 Artificial neural network

Artificial neural networks (ANNs) are a branch of artificial intelligence. A multi-layer perceptron (MLP) is one type of neural network. Unlike other statistical techniques, the MLP makes no prior assumptions concerning the data distribution. It can model highly non-linear functions and can be trained to generalise the results accurately when presented with new and unseen data (Gardner and Dorling, 1998).

A suitable set of connecting weights and transfer functions will make the MLP approximate any smooth, measurable function between the input and output vectors (Hornik et al., 1989). The learning process of the MLP is called training, which requires a set of training data (a series of input and associated output data). These training data are repeatedly presented to the MLP, and the weights in the network are adjusted until the error between actual and desired output is the lowest. The set of optimal weights determined by the

training process will then be applied on the validation set that has not participated in their elaboration (Delon et al., 2007). Once trained with suitably representative training data, the MLP can generalize to new, unseen input data (Gardner and Dorling, 1999). The quality of these processes is assessed through the calculation of training, validation and generalization costs.

The ANN used in this study is based on a commercial version of the Neuro One 5.0<sup>®</sup> 12 software (Netral, Issy les Moulineaux, France). Some details concerning this specific study are given in this paragraph and in Supplement S1. The whole description of the methodology is detailed in Delon et al. (2007). The architecture of the MLP (deduced from the Vapnik–Chervenenkis theory; Vapnik, 1995) is composed of three hidden neurons. All inputs and output are normalized and centred in order to avoid an artefact in the training process. After normalization, the data have the same order of magnitude. The network is used in a static version where the lines of the database are independent of each other.

In this study, an ANN was used to find the best non-linear regression between ebullition fluxes and relevant environmental variables. The database of raw data was composed of 4811 individual ebullition fluxes. Fluxes from a given station measured the same day and at the same depth were averaged (different fluxes with the same depth value and the same meteorological data would introduce noise rather than relevant information into the network), leading to a final database for ANN composed of 510 lines and 4 columns (1 output and 3 inputs; see the discussion paragraph for the choice of the inputs). The data set used by the MLP is separated into two pools, the training one (330 lines) and the validation one (180 lines).

Weight values associated with each input are modified 100 times (the optimization process). Ten initializations (10 series of different sets of weights) are tested for each model. This configuration (100 modifications of weights, 10 models) is tested several times, in order to avoid a local minimum solution. The best algorithm within the 10 launched is chosen by assessing the following criteria: (1) the lowest generalization cost is chosen, (2) the root mean square error (RMSE) of the training set has to be close to the RMSE of the validation set (23.09 and 23.83 in our case), and (3) results giving negative fluxes are discarded. The learning (training) cost is 6.79, the validation cost is 6.9, the generalization cost is 7.47, and the homogeneity is 0.93, which are considered to be good enough criteria for choosing the equation. The equation, coefficients and weights necessary for calculating the ebullition flux are listed in the Supplement section, and in Tables S2 and S3.

### 3.7 Statistical analysis

The methodological, spatial and temporal differences in the CH<sub>4</sub> emissions (diffusive, ebullitive and total emissions) were explored. Differences between groups of data were

examined using either a *t* test or an analysis of variance (ANOVA) in GraphPad Prism (GraphPad Software, Inc., v5.04). The choice of the parametric and non-parametric tests (the Mann–Whitney or Kruskal–Wallis tests compare median values) was dependent on normal and non-normal behaviour of the data sets. The potential spatial variability of ebullitive fluxes was explored in three flooded soil and vegetation clusters: (1) dense forest, which includes dense and medium forest, (2) degraded forest, which includes light and degraded forest, and (3) agricultural lands. The effect of depth on ebullition was also tested according to the following three depth ranges: shallow (0.4–3 m), intermediate (3–6 m) and deep (6–16 m) zones. Finally, CH<sub>4</sub> emissions from the different seasons (WD, WW and CD) were compared in order to evaluate the temporal variability. All statistical tests used a significance level of 5 %. The distributions of the volume of gas emitted by ebullition ( $V_{EB}$ ), CH<sub>4</sub> bubble concentration and flux ( $E_{FUN}$ ) were characterized using the Anderson–Darling goodness of fit in the EasyFit 5.5 trial version. A multi-linear regression (MLR) was used to find the linear relationship between ebullition fluxes and other environmental variables. The MLR used in this study was based on SPSS 15.0 for Windows.

### 3.8 Reservoir water temperature, meteorological and hydrological variables

The temperature at the bottom of the reservoir has been monitored on a fortnightly basis at nine sampling stations in the reservoir, from January 2009 to the present. Meteorological (wind speed, atmospheric pressure, atmospheric temperature, relative humidity, wind direction and net radiation) and hydrological data (rainfall and reservoir water level) were obtained from the monitoring conducted by Electricité de France and Nam Theun 2 Power Company Ltd. (NTPC).

## 4 Results and discussion

### 4.1 Assessment of CH<sub>4</sub> emissions at the reservoir surface by different methods

The effectiveness of four methods (EC, FC, funnels and TBL) in measuring CH<sub>4</sub> emissions at the water–air interface was explored during four field campaigns at NT2 (Table 1). Using these methods, different emission terms were estimated: (1) diffusion ( $D_{GC}$ ,  $D_{GA}$  and  $D_{TBL}$ ) at the water–air interface from  $FC_{GC}$ ,  $FC_{GA}$  and TBL (Supplement Fig. S2a), (2) ebullition ( $E_{FUN}$ ,  $E_{GA}$ ) from funnels and  $FC_{GA}$  (Supplement Fig. S2b), and (3) the sum of diffusion + ebullition ( $DE_{EC}$  and  $DE_{GC}$ ) emissions from EC and  $FC_{GC}$  (Supplement Fig. S2c). All methods were only used simultaneously in March 2011 (Supplement Fig. S2 and Table 1). No matter which method was used or which pathway was measured, the reservoir emitted CH<sub>4</sub> into the atmosphere during the study period (Table 1).

#### 4.1.1 Diffusive emission

Only 30 % of the diffusive fluxes ( $D_{GC}$ ) measured by the  $FC_{GC}$  fulfilled the acceptance criterion ( $r^2 < 0.8$ ) during the four field campaigns. No fluxes were accepted in March 2011, when the water level of the reservoir was decreasing, and only 5 % in June 2011, when the water level was at its lowest. In March 2011, 48 % of the  $D_{GA}$  were accepted. The comparison of the acceptance percentages in March 2011 indicates that short-term deployment of chambers (5 min for  $FC_{GA}$  versus 45 min for  $FC_{GC}$ ) limits the risk of a contamination of the measurement by ebullition. Overall, the average  $D_{GC}$  is  $1.6 \pm 1.1 \text{ mmol m}^{-2} \text{ d}^{-1}$ , which is comparable to the average  $D_{TBL}$  of  $1.4 \pm 2.0 \text{ mmol m}^{-2} \text{ d}^{-1}$  (Tables 1 and 2) for the four field campaigns. For all campaigns except June 2011 (only one validated measurement), the  $D_{TBL}$  calculations were not significantly different from the diffusive fluxes measured with FC (*t* test,  $p < 0.05$ ; details in Table 2). Combining all diffusive fluxes obtained by different approaches (Table 1), our results showed that there is no seasonal variation for the diffusive fluxes measured (*t* test,  $p < 0.05$ ).

#### 4.1.2 Methane ebullition

The CH<sub>4</sub> ebullition was measured with funnels ( $E_{FUN}$ ) in May 2009 and March and June 2011. In March 2011, ebullition (noted  $E_{GA}$ ) was also determined using an  $FC_{GA}$  (Table 1 and Supplement Fig. S2b). One of the major differences between these two methods is the duration of the measurement.  $E_{FUN}$  measurements were performed over 24–48 h periods, whereas  $E_{GA}$  measurements were conducted for 5–20 min only. In June 2011,  $E_{FUN}$  ( $28.0 \pm 11.0 \text{ mmol m}^{-2} \text{ d}^{-1}$ ) were almost twenty-fold and sevenfold higher than  $E_{FUN}$  in May 2009 and March 2011, respectively (Table 1). In March 2011,  $E_{FUN}$  varied by two orders of magnitude, with an average of  $4.2 \pm 3.6 \text{ mmol m}^{-2} \text{ d}^{-1}$ , which is not statistically different from  $E_{GA}$  during the same field campaign ( $4.6 \pm 7.1 \text{ mmol m}^{-2} \text{ d}^{-1}$ ; Tables 1 and 2). It has to be noted that ebullition was observed in around 50 % of  $FC_{GA}$  deployments.

#### 4.1.3 Total CH<sub>4</sub> emissions

We compare here the two techniques that give access to the total emissions, that is the EC technique and the floating chamber which had captured bubbles ( $DE_{GC}$ ). The individual 30-minute  $DE_{EC}$  fluxes varied by four orders of magnitude during all EC deployments (from 0.02 to  $103 \text{ mmol m}^{-2} \text{ d}^{-1}$ ). On average,  $DE_{EC}$  fluxes varied oppositely with the water depth, with the highest mean flux ( $29 \pm 16 \text{ mmol m}^{-2} \text{ d}^{-1}$ ) in June 2011 for the shallowest water depth ( $\sim 1.5 \text{ m}$ ) (Table 1 and Fig. 3). Supplement Figs. S2c and 3 show total CH<sub>4</sub> fluxes calculated from  $DE_{GC}$



**Table 1.** Comparison of different methods to assess CH<sub>4</sub> emissions. All fluxes are in mmol m<sup>-2</sup> d<sup>-1</sup> (average ± standard deviation), and the number of measurements (*n*) is given between brackets.

	Diffusion D		Ebullition E		Diffusion+Ebullition DE			
	Method	Average ± SD ( <i>n</i> )	Method	Average ± SD ( <i>n</i> )	Method	Average ± SD ( <i>n</i> )	Method	Average ± SD ( <i>n</i> )
May 09	D <sub>GC</sub> <sup>1</sup>	1.2 ± 0.8 (12)	E <sub>FUN</sub> <sup>2</sup>	1.6 ± 2.9 (9)	DE <sub>EC</sub> <sup>3</sup>	6.5 ± 3.3 (39)	DE <sub>EC</sub>	6.9 ± 2.6 (2)
	D <sub>GGA</sub> <sup>4</sup>	NA	E <sub>GGA</sub> <sup>5</sup>	NA	DE <sub>GC</sub> <sup>6</sup>	1.9 ± 2.3 (16)	E <sub>FUN</sub> +D <sub>GGA</sub>	2.8 ± 1.6 (2)
	D <sub>TBL</sub> <sup>7</sup>	1.5 ± 2.2 (14)					E <sub>FUN</sub> +D <sub>TBL</sub>	3.1 ± 1.7 (2)
Mar 10	D <sub>GC</sub>	0.9 ± 0.5 (9)	E <sub>FUN</sub>	NA	DE <sub>EC</sub>	5.8 ± 5.0 (138)	DE <sub>EC</sub>	5.7 ± 3.7 (14)
	D <sub>GGA</sub>	NA	E <sub>GGA</sub>	NA	DE <sub>GC</sub>	8.4 ± 17.5 (24)		
	D <sub>TBL</sub>	1.3 ± 0.8 (12)						
Mar 11	D <sub>GC</sub>	NA	E <sub>FUN</sub>	4.2 ± 3.6 (95)	DE <sub>EC</sub>	7.2 ± 2.9 (105)	DE <sub>EC</sub>	7.2 ± 0.8 (4)
	D <sub>GGA</sub>	1.9 ± 1.2 (28)	E <sub>GGA</sub>	4.6 ± 7.1 (30)	DE <sub>GC</sub>	8.9 ± 10.5 (58)	E <sub>FUN</sub> +D <sub>GGA</sub>	6.1 ± 1.2 (4)
	D <sub>TBL</sub>	1.1 ± 2.0 (52)					E <sub>FUN</sub> +D <sub>TBL</sub>	5.3 ± 1.2 (4)
Jun 11	D <sub>GC</sub>	1.5 (1)	E <sub>FUN</sub>	28.0 ± 11.0 (126)	DE <sub>EC</sub>	29.1 ± 16.4 (133)	DE <sub>EC</sub>	26.6 ± 6.7 (5)
	D <sub>GGA</sub>	NA	E <sub>GGA</sub>	NA	DE <sub>GC</sub>	54.3 ± 35.0 (21)	E <sub>FUN</sub> +D <sub>TBL</sub>	29.9 ± 5.5 (5)
	D <sub>TBL</sub>	1.9 ± 2.5 (19)						
All	D <sub>GC</sub>	1.1 ± 0.7 (22)	E <sub>FUN</sub>	17.1 ± 14.7 (230)	DE <sub>EC</sub>	13.6 ± 14.5 (415)	DE <sub>EC</sub>	16.0 ± 11.1 (11)
	D <sub>GGA</sub>	1.9 ± 1.2 (28)	E <sub>GGA</sub>	4.6 ± 7.1 (30)	DE <sub>GC</sub>	15.8 ± 25.2 (121)	E <sub>FUN</sub> +D <sub>FC</sub>	16.3 ± 13.4 (11)
	D <sub>TBL</sub>	1.4 ± 2.0 (97)					E <sub>FUN</sub> +D <sub>TBL</sub>	16.3 ± 13.8 (11)

D<sub>GC</sub><sup>1</sup>: Diffusion from floating chamber (FC) and post-analysis with gas chromatography. E<sub>FUN</sub><sup>2</sup>: Ebullition from submerged funnel. DE<sub>EC</sub><sup>3</sup>: Total emissions measured by eddy covariance. D<sub>GGA</sub><sup>4</sup>: Diffusion from FC and in situ gas analyser. E<sub>GGA</sub><sup>5</sup>: Ebullition from FC and in situ gas analyser. DE<sub>GC</sub><sup>6</sup>: Total emissions by FC (diffusion + ebullition) affected by bubbling. D<sub>TBL</sub><sup>7</sup>: Diffusion calculated by thin boundary layer (TBL) method from surface CH<sub>4</sub> concentrations.

**Table 2.** Statistical test for the comparison of different methods to assess CH<sub>4</sub> emissions. The difference is significant if *p* < 0.05.

	May 09	Mar 10	Mar 11	Jun 11	All
D <sub>TBL</sub>	D <sub>GC</sub> 0.6027	D <sub>GC</sub> 0.2815	D <sub>GC</sub> 0.0513	D <sub>GC</sub> –	D <sub>GC</sub> 0.5049
DE <sub>GC</sub>	DE <sub>EC</sub> < 0.0001	DE <sub>EC</sub> 0.0129	DE <sub>EC</sub> 0.1075	DE <sub>EC</sub> < 0.0001	DE <sub>EC</sub> 0.0004
E <sub>FUN</sub> +D <sub>GGA</sub>			0.2021		
E <sub>FUN</sub> +D <sub>GC</sub>	0.2222	–	–	–	0.5114
E <sub>FUN</sub> +D <sub>TBL</sub>	0.2533	–	0.057	0.8413	0.3933

data. Altogether, DE<sub>GC</sub> also varied by four orders of magnitude (from 0.02 to 132 mmol m<sup>-2</sup> d<sup>-1</sup>) during all deployments, and DE<sub>GC</sub> fluxes also varied oppositely with the water depth, with the highest mean flux (54 ± 35 mmol m<sup>-2</sup> d<sup>-1</sup>) in June 2011. For half of the campaigns, DE<sub>GC</sub> and DE<sub>EC</sub> were significantly different (Table 2 and Fig. 3).

We then compared continuous DE<sub>EC</sub> to the sum of the discrete sampling of diffusive (D<sub>GC</sub>, D<sub>GGA</sub> and D<sub>TBL</sub>) and ebullitive (E<sub>FUN</sub> and E<sub>GGA</sub>) fluxes for three field campaigns (May 2009, March and June 2011) of four (no ebullition measurements taken within the footprint in March 2010). The

sum of independent estimates of diffusive (D<sub>TBL</sub>, D<sub>GC</sub>, D<sub>GGA</sub>) and ebullitive (E<sub>FUN</sub> and E<sub>GGA</sub>) fluxes determined on less than 1 m<sup>2</sup> were found to be in good agreement with total emissions determined from EC over thousands of m<sup>2</sup> (Table 2 and Fig. 3). This confirms that the EC system is able to pick up both diffusive and ebullitive fluxes from the reservoir, as already shown by Schubert et al. (2012).

Even if statistically the comparison of total emissions by the different approaches is good, one should note that, on a handful of occasions, DE<sub>GC</sub> exceeds DE<sub>EC</sub> and the sum of diffusive fluxes (D<sub>GC</sub>, D<sub>GGA</sub> and D<sub>TBL</sub>) and ebullition (E<sub>FUN</sub> and E<sub>GGA</sub>) by a factor of up to 100 (Supplement Fig. S2c). These differences can clearly be explained by the sudden release of bubbles on these rare occasions. This reveals very strong spatial and temporal heterogeneities of the ebullition process. Because ebullition is highly sporadic and occurs during a very short period of time (Varadharajan and Hemond, 2012), its measurement by FC over a short period of time and a small surface might lead to an over-estimation of this emission pathway if hot spots and hot moments are captured during the deployment of the chamber. Such a phenomenon is strongly smoothed when using funnels over longer periods of time than the typical



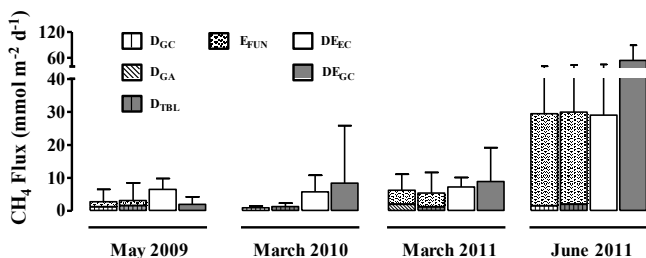


**Figure 3.** Inter-comparison of the estimates of CH<sub>4</sub> emissions obtained using the variety of methods deployed during the four field campaigns. Note that no ebullition was measured in March 2010. D<sub>GC</sub>: Diffusion from the floating chamber (FC) and post-analysis with gas chromatography. D<sub>TBL</sub>: Diffusion calculated by the thin boundary layer (TBL) method from surface CH<sub>4</sub> concentrations. D<sub>GA</sub>: Diffusion from FC and the in situ gas analyser. E<sub>FUN</sub>: Ebullition from submerged funnel. E<sub>GA</sub>: Ebullition from FC and the in situ gas analyser. DE<sub>EC</sub>: Total emissions measured by eddy covariance. DE<sub>GC</sub>: Total emissions by FC (diffusion + ebullition) affected by ebullition.

floating chamber deployment time (typically 12–48 h versus 10–45 min). Globally the EC measurements are ideal for capturing the large spatial and temporal variability of total CH<sub>4</sub> fluxes at the surface of aquatic ecosystems prone to ebullition. However, the discrimination of diffusive fluxes and ebullition requires the deployment of either bubble-shielded FC to obtain the diffusive emissions or the deployment of funnels to obtain the ebullition. The use of recent techniques like the equilibrator technique (Abril et al., 2006) and subsequent TBL calculations for diffusive fluxes, or hydroacoustic measurement, which is capable of capturing the hot spots of ebullition (DeSontro et al., 2011), combined with the EC, might also allow the identification of those hot moments and their controlling factors.

For the four campaigns, the contribution of ebullition to total emissions from EC (DE<sub>EC</sub>) ranged between 57 and 93 % of the total CH<sub>4</sub> emissions from the EC footprint (Table 1 and Fig. 3). As already mentioned in some recent publications (Bastviken et al., 2004, 2010; DeSontro et al., 2010, 2011; Schubert et al., 2012), ebullition is a major CH<sub>4</sub> pathways that is often neglected in aquatic ecosystems, especially in the tropics and subtropics, where the high temperatures trigger ebullition by both enhancing CH<sub>4</sub> production in the sediments (Duc et al., 2010) and decreasing CH<sub>4</sub> solubility in the water column (Yamamoto et al., 1976).

#### 4.2 Total CH<sub>4</sub> emissions (DE<sub>EC</sub>) versus hydrostatic pressure

Based on the four field campaigns time series from the EC system (Supplement Fig. S3), we did not find any correlation between DE<sub>EC</sub> and the wind speed and the buoyancy fluxes (Supplement Fig. S4). As these parameters are known controlling factors of the diffusive fluxes (e.g. Guérin et al.,

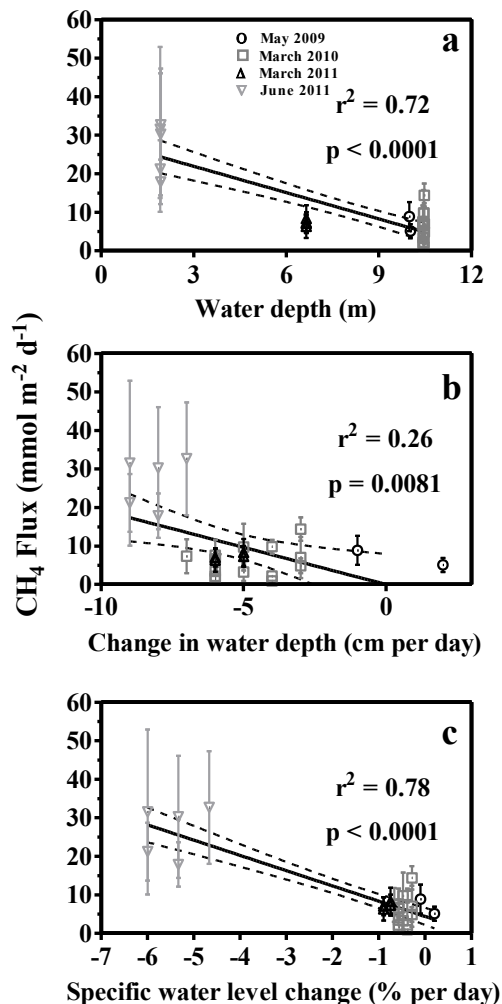


**Figure 4.** CH<sub>4</sub> emissions measured by eddy covariance (DE<sub>EC</sub>) versus (a) water depth, (b) change in water depth, and (c) specific water level change for the four field campaigns. Note that turbines were not started in May 2009, leading to no water level change during that field campaign. In all panels, the solid line is the regression line and the dash lines represent the confidence interval.

2007; MacIntyre et al., 2010), the absence of correlation indirectly confirms that ebullition dominates the total emissions at the surface of the NT2 Reservoir, as shown in the previous section.

Daily DE<sub>EC</sub> was plotted against the daily (1) water depth and (2) change in the water depth (cm d<sup>-1</sup>), and (3) specific water level change (water level change normalized by the average water depth) (Fig. 4). DE<sub>EC</sub> is negatively correlated with the water depth ( $p < 0.0001$ , Fig. 4a), as is usually the case for ebullition in lakes (Bastviken et al., 2004; Wik et al., 2013), hydroelectric reservoirs (Galy-Lacaux et al., 1999; Keller and Stallard, 1994), estuaries (Chanton et al., 1989) and the marine environment (Algar and Boudreau, 2010, Martens and Val Klump, 1980). According to our data set, emissions can be enhanced by a factor of 5 for a water

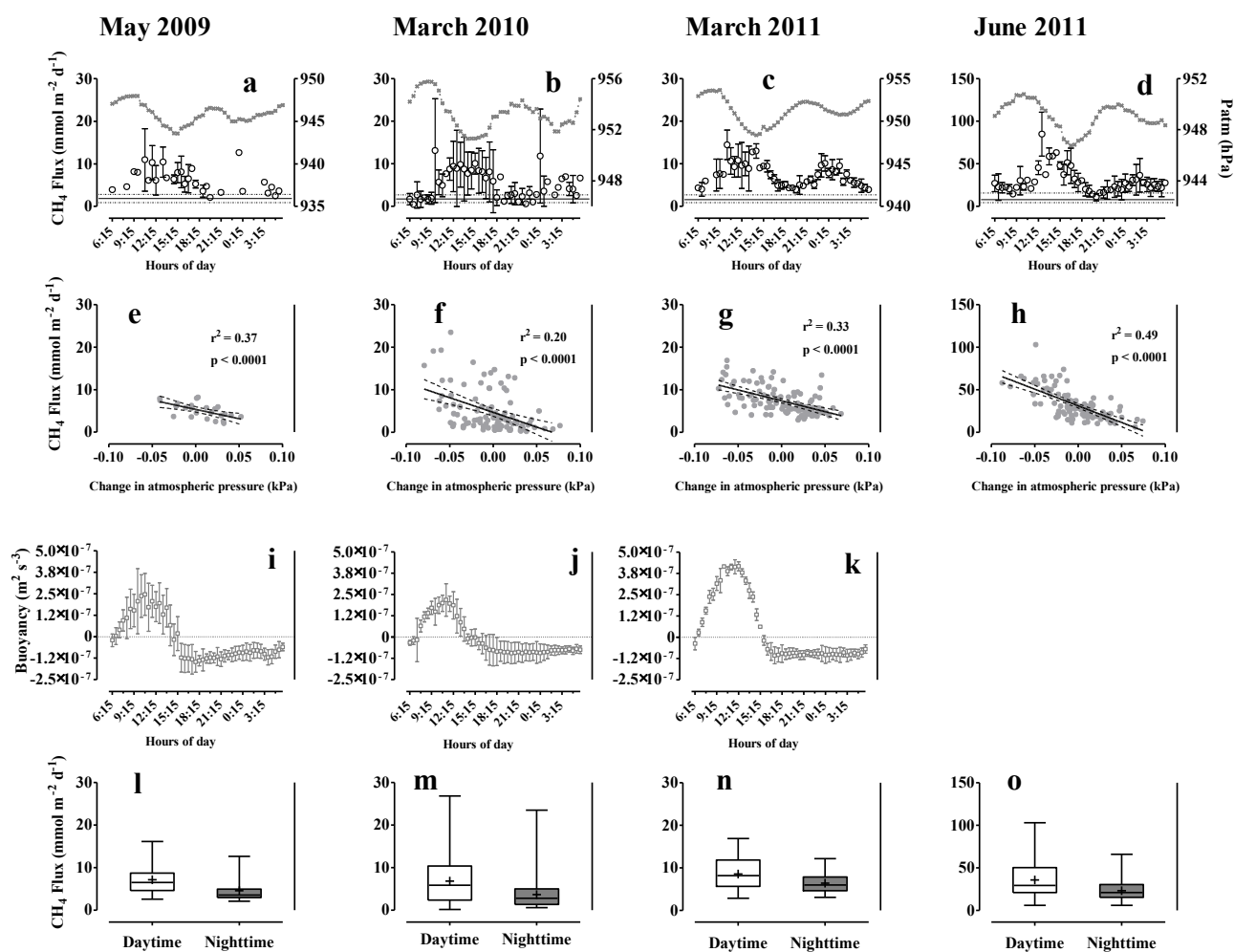


**Figure 5.** (a, b, c, d): 30 mn-binned CH<sub>4</sub> emissions measured by eddy covariance (DE<sub>EC</sub>) (circle) and 30 mn-binned atmospheric pressure (cross) for the four field campaigns. (e, f, g): 30 mn-binned buoyancy flux (note that the June 2011 data are not available). (h, i, j, k): Individual 30 min CH<sub>4</sub> emissions measured by eddy covariance (DE<sub>EC</sub>) versus change in the atmospheric pressure for the four field campaigns. (l, m, n, o): Nighttime and daytime range for CH<sub>4</sub> emissions measured by eddy covariance (DE<sub>EC</sub>) for the four field campaigns. Note that the y axis scale differs for the June 2011 campaign (d, k, o). In panels e–h, the solid line is the regression line and the dash lines represent the confidence interval.

depth difference of 10 m, which corresponds to the observed maximum seasonal water level variations at NT2. Though measured in different seasons, diffusive fluxes measured by FC in the EC footprint are constant for the four deployments (see Table 1). This implies that seasonal variation in the CH<sub>4</sub> emissions at a single site is mostly controlled by water level differences and subsequent ebullition. However, this does not exclude the possibility that CH<sub>4</sub> emissions are higher during the warm dry season than during cooler seasons as a consequence of enhanced methanogenesis with higher temperature (Duc et al., 2010). It appears that the effect of water level change (6–9 cm) is proportionally stronger in shallow water (2 m) than in deep water (10.5 m) (June 2011, Fig. 4b), meaning that the same water level change could favour higher fluxes in shallow areas than in deep waters. This effect is well

described by the specific water level change (Fig. 4c): fluxes were lower when daily variations in the depth were 5–7 cm, corresponding to specific water level changes of less than 1 % for most of the field campaigns (March 2010 and 2011 rather than in June 2011), when the same water level variations corresponded to a specific water level change of 4–5 % which triggered emissions of up to 100 mmol m<sup>-2</sup> d<sup>-1</sup>. Overall, in the context of this subtropical hydroelectric reservoir with a high contribution of ebullition, these results show that the hydrostatic pressure plays an important role in controlling the CH<sub>4</sub> fluxes, since (1) the water depth explains about 70 % (Fig. 4a) of the variability of the CH<sub>4</sub> emissions, (2) seasonal variations in CH<sub>4</sub> emissions by a factor of 5 are mostly due to the enhancement of ebullition due to the low water level in the WD season, and (3) the effect of a change in water level

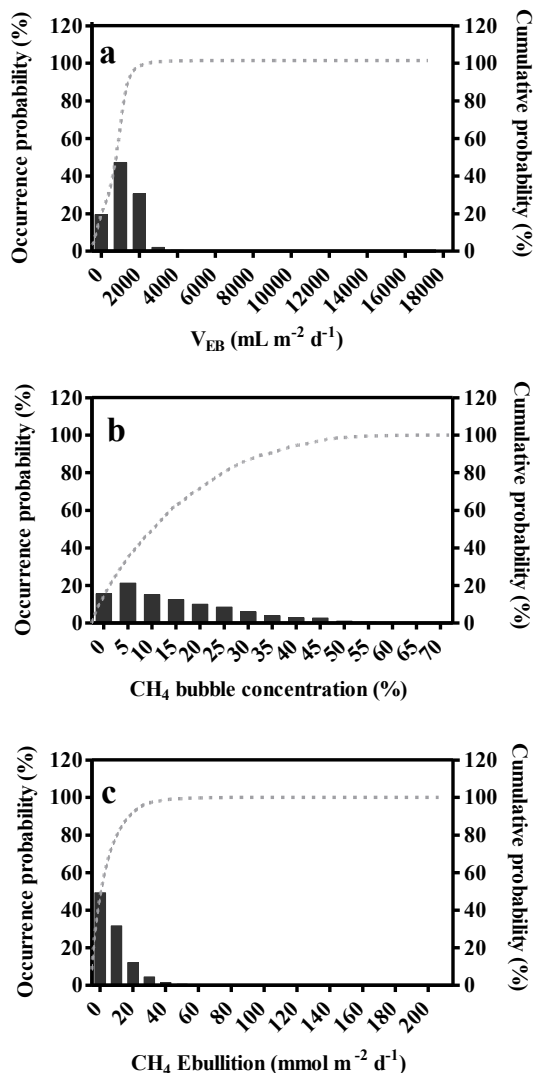


**Figure 6.** Histograms showing the distribution of (a) the ebullition rate, (b) the CH<sub>4</sub> bubble concentration, and (c) the ebullition measured by funnels.

on ebullition is more effective in shallow areas than in the deeper zone of aquatic ecosystems.

#### 4.3 Effect of atmospheric pressure on diurnal cycle of total CH<sub>4</sub> emissions ( $DE_{EC}$ )

In the  $DE_{EC}$  time series (Supplement Fig. S3), it appeared that two CH<sub>4</sub> peaks of emissions occurred daily. In order to investigate the drivers of these emission peaks,  $DE_{EC}$  flux data were binned by time of the day and then averaged for each deployment. A clear diurnal bimodal pattern of  $DE_{EC}$  fluxes, with a first peak in the middle of the night (between midnight and 3:00 a.m.) and a second one around noon, was observed during all four campaigns (Fig. 5a, b, c, d), and is apparently related to the semidiurnal evolution of the atmospheric pressure (a phenomenon due to global atmospheric

tides). The diurnal pattern of CH<sub>4</sub> emissions was also recently evidenced by Sahlée et al. (2014), who measured CH<sub>4</sub> fluxes using an EC system over a natural lake in Sweden. They observed higher fluxes at nighttime linked to enhanced diffusion through convective mixing (MacIntyre et al., 2010; Sahlée et al., 2014). At NT2, 30 min-binned  $DE_{EC}$  is anti-correlated with atmospheric pressure (Fig. 5a, b, c, d). Furthermore,  $DE_{EC}$  was found to be anti-correlated with the change in atmospheric pressure, evidencing a strong control of the atmospheric pressure change over the fluxes, most likely through ebullition (Fig. 5e, f, g, h). It is noteworthy to point out that the coefficient of determination is better for the campaign with the lower water depth at the EC site (1.5 m, June 2011, Fig. 5e, f, g, h), indicating that the variations in the atmospheric pressure have more effect at low hydrostatic pressure (higher relative change in pressure). We also calculated buoyancy fluxes in order to look for the potential occurrence of high diffusive fluxes due to convective mixing (Fig. 5i, j, k), as in MacIntyre et al. (2010) and Sahlée et al. (2014). On the one hand, the nighttime peak of CH<sub>4</sub> emissions coincides with low but constant buoyancy fluxes (i.e. the most unstable water column) and moderate atmospheric pressure drop. The fact that the buoyancy flux does not decrease during the peak of CH<sub>4</sub> indicates a low control on the emissions, if any. On the other hand, daytime peaks of CH<sub>4</sub> emissions are linked to maximum buoyancy fluxes, which cannot enhance emissions (i.e. the most stable water column). These observations tend to prove that CH<sub>4</sub> bursts in the night and around noon (up to  $100 \text{ mmol m}^{-2} \text{d}^{-1}$ ) could be attributed entirely to the atmospheric pressure drops that triggered ebullition, more than any buoyancy effect.

The effect of pressure on ebullition was already shown in natural lakes (Casper et al., 2000; Eugster et al., 2011; Mattson and Lickens, 1990; Wik et al., 2013) and peatlands (Fechner-Levy and Hemond, 1996; Tokida et al., 2005), as well as the effect of buoyancy fluxes on diffusive fluxes in lakes (MacIntyre et al., 2010; Sahlée et al., 2014), but this is the first time that a daily bimodal variation in CH<sub>4</sub> emissions is evidenced. CH<sub>4</sub> emissions around noon were approximately 10 times higher than fluxes near sunset and sunrise (Fig. 5l, m, n, o), and 2 times higher than during the nighttime for all EC deployments ( $p = 0.0036$ ,  $p = 0.0002$ ,  $p = 0.0015$  and  $p < 0.0001$ , respectively for May 2009, March 2010, March 2011 and June 2011; Mann–Whitney test). This implies that the quantification of CH<sub>4</sub> emissions by ebullition and diffusion from inland aquatic ecosystems has to be done over 24 h cycles in order to obtain realistic estimates.

#### 4.4 Spatio-temporal variations in CH<sub>4</sub> ebullition ( $E_{FUN}$ )

By definition, EC systems are not suitable for the exploration of fine spatial variations and the effect of water depth on ebullition within a single season. Because of logistic difficulties, it was not possible to leave the EC system on site for a full

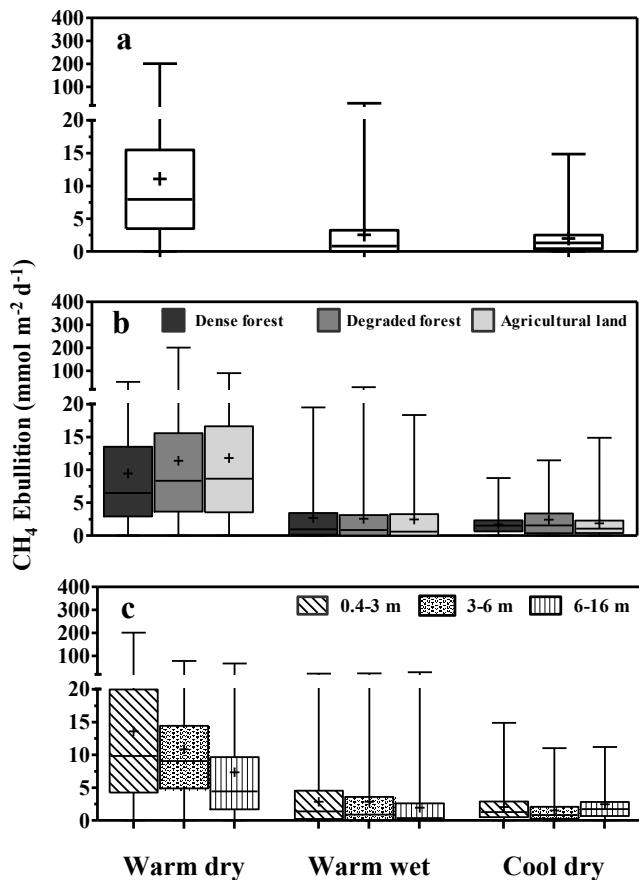


**Figure 7.** Ebullition measured by funnels for (a) the three different seasons, (b) the three major different flooded ecosystems (dense/medium forest, light/degraded forest, and agricultural land), and (c) three depth zones.

year. As a matter of consequence, we also deployed funnels at seven stations every week (4811 measurements) in order to explore the spatial and temporal variability of ebullition, and to identify its controlling factors.

The volume of emitted gas  $V_{EB}$  averaged  $1205 \text{ mL m}^{-2} \text{ d}^{-1}$  and ranged from 0 to  $17587 \text{ mL m}^{-2} \text{ d}^{-1}$ . The positively skewed hyperbolic secant distributions ( $\alpha = 782.41$  and  $\mu = 1205$ ; Fig. 6a) of  $V_{EB}$  showed that, for most of the records of ebullition ( $\sim 97\%$ ),  $V_{EB}$  was below  $2000 \text{ mL m}^{-2} \text{ d}^{-1}$ . The  $V_{EB}$  in the WW season (median =  $732 \text{ mL m}^{-2} \text{ d}^{-1}$ ) was statistically different ( $p < 0.0001$ , Kruskal–Wallis test) and almost two times lower than in the WD (median =  $1330 \text{ mL m}^{-2} \text{ d}^{-1}$ ) and CD (median =  $1254 \text{ mL m}^{-2} \text{ d}^{-1}$ ) seasons.

CH<sub>4</sub> concentration in the bubbles ranged from 0.001 to 69.2%, and most of the time was lower than 30% (Fig. 6b). The average concentration was 14.9%, that is two- to six-fold lower than the concentrations reported for subarctic lakes ( $34.8 \pm 25.2\%$ , Wik et al., 2013), Siberian thermokarst lakes ( $82 \pm 7\%$ , Walter et al., 2008), open wa-

ter and vegetated sites in a beaver pond ( $47.2 \pm 20.8\%$  and  $26.6 \pm 12.4\%$ ; Dove et al., 1999), and tropical reservoirs (59–66%, DelSontro et al., 2011). However, the mean CH<sub>4</sub> concentration in bubbles at NT2 is similar to the concentration observed in rice paddies and vegetated wetlands (Rothfuss and Conrad, 1992; Frenzel and Karofeld, 2000; Krüger et al., 2002; Chanton et al., 1989; Tyler et al., 1997) and well-oxygenated streams (Crawford et al., 2014). The CH<sub>4</sub> concentrations in bubbles in these ecosystems are supposed to be low because of high methanotrophic activity in the rhizosphere of the vegetation permitted by high ventilation of the soils by active transport of air through the stems of the vegetation. In the NT2 Reservoir, there is almost no aquatic vegetation rooted in the littoral zone of the reservoir. However, the reservoir floods very compacted soils. As a consequence, bubbles might develop close to the flooded soil/sediment–water interface. The area where bubbles were collected has a maximum depth close to the depth of the oxycline for most of the year (4–7 m), which implies that the first millimetres of the flooded soils are probably oxygenated in the area shallower than 10 m. In addition, during the lake overturn in the CD season and during the sporadic destratification events in the WW season, O<sub>2</sub> could reach the flooded soil–water interface. CH<sub>4</sub> oxidation could therefore affect the CH<sub>4</sub> concentration in bubbles in the flooded soils before they escape, leading to a low concentration of CH<sub>4</sub> in bubbles. The statistical test ( $p < 0.0001$ , Kruskal–Wallis test) suggested that the CH<sub>4</sub> concentrations in bubbles differed significantly seasonally, with CH<sub>4</sub> concentrations 3–5 times higher during the WD season ( $19.27 \pm 12.43\%$ ), when the oxygen penetration in the water column is at a minimum, than during the WW ( $7.30 \pm 8.78\%$ ) and CD ( $4.57 \pm 5.78\%$ ) seasons. In addition to a potential role of CH<sub>4</sub> oxidation, the effect of temperature on both the CH<sub>4</sub> solubility and the methanogenesis might have influenced the seasonal variations in the CH<sub>4</sub> bubble content. The bubble CH<sub>4</sub> concentration in the WW season ranged from 0.001 to 49%, and was similar whatever the depth of the water column ( $p = 0.08$ , Kruskal–Wallis test), whereas bubble CH<sub>4</sub> concentrations differed among depth zones in the WD and CD seasons ( $p < 0.0001$  (WD) and  $p = 0.0054$  (CD)). In the WD season, the bubble CH<sub>4</sub> concentration was two times higher in the shallowest (median = 21.52%) than in the deepest zones (12.78%). According to McGinnis et al. (2006) and Ostrovsky et al. (2008), the decrease in the CH<sub>4</sub> concentration in bubbles by the dissolution of CH<sub>4</sub> for a maximum water depth of 10 m can reach up to 20%. This process could therefore explain the variation in CH<sub>4</sub> concentration in bubbles according to depth. Overall, we show that the CH<sub>4</sub> concentrations in bubbles vary seasonally and spatially by five orders of magnitude at the NT2 Reservoir, suggesting that precise extrapolation of the ebullition must take into account both the volume of gas released by the sediments at high resolution (e.g. DelSontro et al., 2010) and the high variability in CH<sub>4</sub> concentrations in the bubbles.

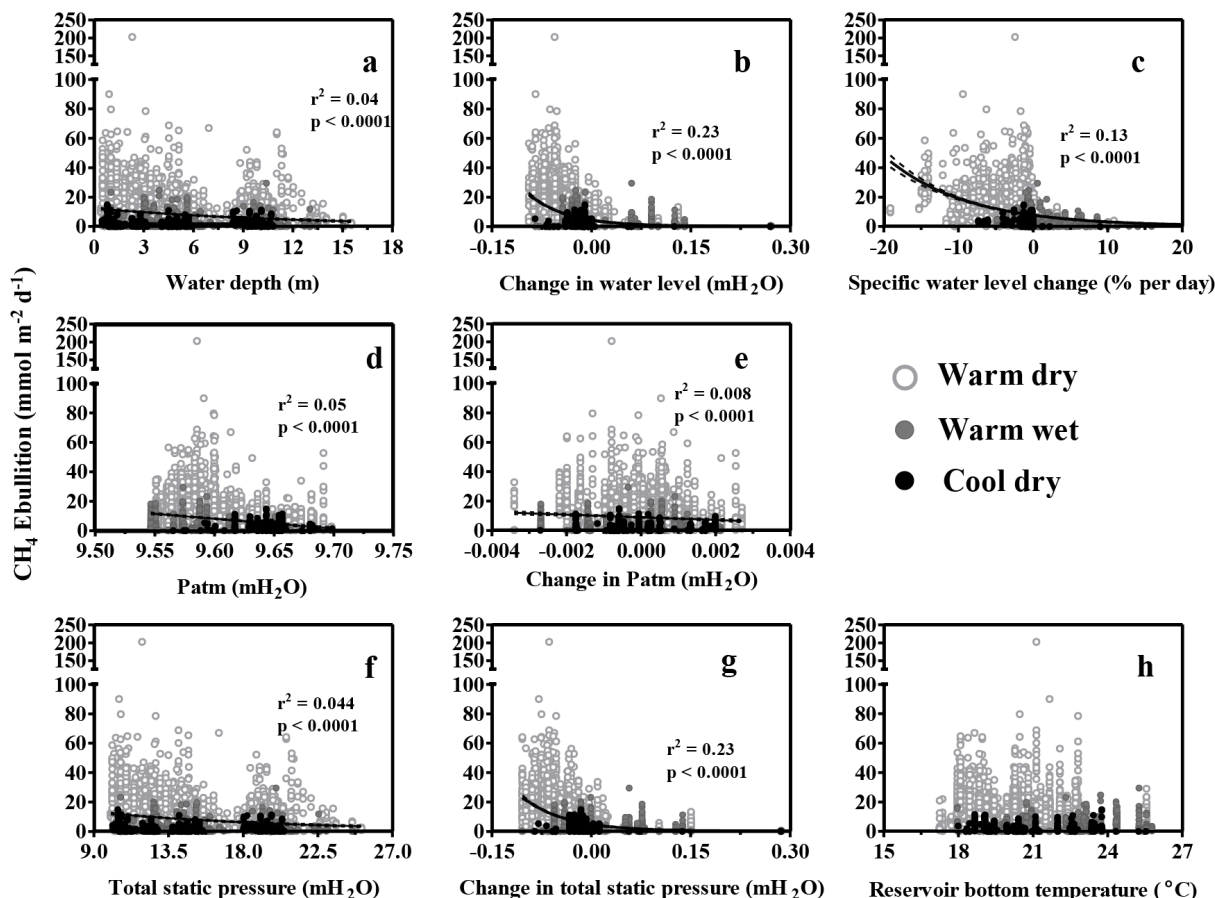


**Figure 8.** Ebullition measured by funnels versus (a) water depth, (b) change in water level, (c) specific water level change, (d) atmospheric pressure, (e) change in atmospheric pressure, (f) total static pressure, (g) change in total static pressure, and (h) reservoir bottom temperature.

Like  $V_{EB}$  and bubble CH<sub>4</sub> concentrations,  $E_{FUN}$  fluxes varied by five orders of magnitude at the NT2 Reservoir, and showed large variability (the coefficient of variation is 122 %). However, the  $E_{FUN}$  distribution shows that 95 % of the ebullition records were below 25 mmol m<sup>-2</sup> d<sup>-1</sup> (Fig. 6c). On average, ebullition was  $8.5 \pm 10.5$  mmol m<sup>-2</sup> d<sup>-1</sup> and ranged from 0 to 201.7 mmol m<sup>-2</sup> d<sup>-1</sup>. At NT2, ebullition is in the lower range of ebullition reported for tropical reservoirs (Abril et al., 2005; DelSontro et al., 2011; dos Santos et al., 2006; Galy-Lacaux et al., 1999; Keller and Stallard, 1994). Ebullition was ten times higher in the WD season (median = 7.9 mmol m<sup>-2</sup> d<sup>-1</sup>) than in the WW (median = 0.81 mmol m<sup>-2</sup> d<sup>-1</sup>) and CD (median = 1.3 mmol m<sup>-2</sup> d<sup>-1</sup>) seasons (Fig. 7a). This might be related to the potential dependency of CH<sub>4</sub> solubility and production on temperature, and to the dependency of ebullition on water depth and change in water depth as explained before. Ebullition from flooded dense forest, degraded forest and agricultural lands was similar during the WW and CD seasons ( $p = 0.1077$  (WW) and  $p = 0.2324$  (CD), Kruskal–Wallis test; Fig. 7b), but slightly lower in the dense forest (median = 6.46 mmol m<sup>-2</sup> d<sup>-1</sup>) than in the

degraded forests (median = 8.3 mmol m<sup>-2</sup> d<sup>-1</sup>) and agricultural lands (8.63 mmol m<sup>-2</sup> d<sup>-1</sup>) during the WD season. The ebullition dependency on water depth varies with season (Fig. 7c). Ebullition decreases significantly with depth in the WD season, whereas that decrease was not significant for the low emissions of the CD season. This implies that the annual extrapolation of ebullition must account for the seasonal evolution of the ebullition versus depth relationship.

#### 4.5 Controlling factors on CH<sub>4</sub> ebullition ( $E_{FUN}$ )

According to our results on short-term variation in ebullition obtained from EC and previous works based on both EC and funnels, ebullition fluxes were plotted against water level, water level change, specific water level change, atmospheric pressure, change in atmospheric pressure and bottom temperature. The high scatter in different regressions between ebullition and the controlling factors is likely due to the fact that ebullition is controlled by a combination of all those factors (Fig. 8). The effects of both water depth and the atmospheric pressure were combined by calculating the total static pressure (TSP) and the change in TSP in mH<sub>2</sub>O at the bottom

of the reservoir, which is the sum of atmospheric and hydrostatic pressure changes. These two parameters were then correlated with ebullition using an exponential decrease regression model (Fig. 8f, g).

Ebullition decreased from 203 to 0 mmol m<sup>-2</sup> d<sup>-1</sup> for water depths ranging from 0.4 to 16 m (Fig. 8a). The median of all fluxes measured at shallow sites (0.4–3 m: 6.3 mmol m<sup>-2</sup> d<sup>-1</sup>) was almost twofold higher than the median in the deepest zone (6–16 m: 2.9 mmol m<sup>-2</sup> d<sup>-1</sup>). The correlation between depth and ebullition is highly significant ( $p < 0.0001$ ), but still, this parameter alone only explains 4 % of the variation in the ebullition ( $r^2 = 0.04$ ; Fig. 8a). The dependency of ebullition on the depth could be attributed to two physical processes. First, a deeper water column means higher hydrostatic pressure, which could prevent the formation of bubbles by increasing CH<sub>4</sub> solubility in the sediment pore waters. Second, while the CH<sub>4</sub> bubbles escape the sediment, bubbles partly dissolve in the water on their way up to the atmosphere (DelSontro et al., 2010; McGinnis et al., 2006). The percentage of CH<sub>4</sub> dissolution and thereby oxidation increases with the water depth. On the opposite side, shallow zones favour bubble formation because they are generally warmer, which both stimulates methanogenesis (Duc et al., 2010) and makes CH<sub>4</sub> less soluble (Yamamoto et al., 1976).

As seen above, water depth has an impact on ebullition, but it appears that water depth change (or hydrostatic pressure change) has a stronger effect ( $r^2 = 0.23$ ) on this phenomenon. Water depth and hydrostatic pressure decrease trigger ebullition, as demonstrated here (Fig. 8b) and in previous works in marine and estuarine environments, and in freshwater wetlands (Boles et al., 2001; Chanton et al., 1989; Engle and Melack, 2000; Martens and Klump, 1980). During the periods of falling water level, ebullition was five-fold higher (median = 7.5 mmol m<sup>-2</sup> d<sup>-1</sup>) than the ebullition during increasing water level (median = 1.5 mmol m<sup>-2</sup> d<sup>-1</sup>). The correlation shows that the change in the water level alone explains 23 % of the ebullition variability, and it evidences why ebullition is significantly higher during the WD season, when the water level is falling (negative water level change), than during the WW season, when the water level is rising, or during the CD season, when it is stable. The effect of the specific water level change on ebullition (Fig. 8c) is not as high as expected ( $p < 0.0001$ ,  $r^2 = 0.13$ ) on this large data set of funnel measurements encompassing a wider range of environmental conditions and flooded ecosystems compared to what we obtained with the EC-derived data only. However, for a given water depth, water depth change and specific water level change, ebullition was in the same range, regardless of what was obtained from EC or funnels. We hypothesize that EC installed in a zone with a very homogeneous land cover (corresponding to flooded agricultural lands) and covering a large footprint allows us to characterize the controlling factors better than discrete sampling with funnels over a few cm<sup>2</sup> in various types of flooded ecosystems.

The relationship of ebullition obtained with funnels over 24 h versus atmospheric pressure and pressure change were highly significant (Fig. 8d, e), but with very low determination coefficients. These much lower  $r^2$  values compared to the one obtained from the EC could be explained by the fact that mean atmospheric pressure change from one day to the next is smaller than the diurnal variations in atmospheric pressure that we observed during the EC deployments.

The magnitude of the atmospheric pressure varied within a small range (9.55–9.70 hPa, or an equivalent of 0.15 m H<sub>2</sub>O). As a matter of consequence, our attempt to combine the effect of hydrostatic and atmospheric pressure (i.e. the so-called total static pressure or TSP) was not highly convincing, since we did not improve the correlation coefficient using the TSP (Fig. 8f, g) compared to what we observed for the hydrostatic pressure alone.

Finally, we found a very low correlation between ebullition and reservoir bottom temperature ( $r^2 = 0.03$ , Fig. 8h). This shows, given the hydrodynamics and the temperature range experienced in the NT2 Reservoir, that this physical parameter has very low predictive power. This is due to the co-variation of several factors at the same time, hiding a possible effect of temperature on the benthic methanogenesis activity. The absence of a correlation between temperature and ebullition is mostly due to the fact that the highest bottom water temperatures were often synchronized with the beginning of the WW season when the ebullition is moderated by the water level increase. This illustrates the complexity of controlling factors interacting at the same time and with each other in a non-linear way. As a matter of fact, it is worth trying a non-linear method to represent ebullition through several relevant parameters, identified in this section but not necessarily highly correlated with ebullition.

#### 4.6 Extrapolation of ebullition at the NT2 Reservoir scale by ANN

The extrapolation of ebullition from field measurements to the whole NT2 aquatic ecosystem is challenging. In all studies published so far, the average ebullition is multiplied by the surface area of the shallow zone where ebullition was measured (e.g. Abril et al., 2005; Wik et al., 2013), by type of habitat (e.g. Smith et al., 2000) or by a combination of the two approaches (DelSontro et al., 2011). Our data set together with the determination of some major controlling factors of ebullition allowed us an attempt for the first time of the extrapolation of this major CH<sub>4</sub> pathway based on physical processes.

As a first approach, we used multi-linear regressions. We obtained good correlations with the change in the total static pressure. However, we were able to explain only 21 % of the variance in the ebullitive fluxes (data not shown). The relatively low percentage of explained variance revealed that the complexity of the interactions between the controlling factors of the ebullition is only partially resolved through simple



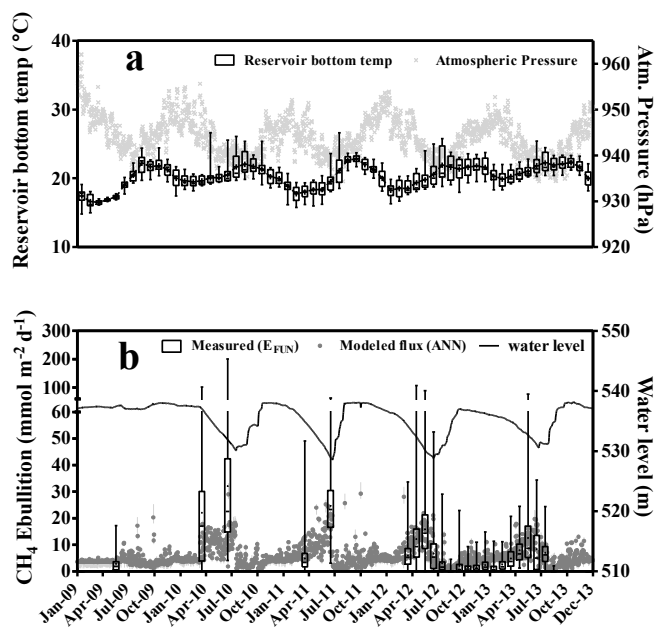


**Figure 9.** Time series of the (a) reservoir bottom temperature and atmospheric pressure, and (b) funnels measured and ANN-modelled ebullition fluxes along with the reservoir water level. In panel (b), the boxes show the median concentration and the interquartile range, and whiskers denote the full range of all values. The plus signs (+) in the boxes of panels (a) and (b) show the mean values.

linear equations. A non-linear approach was used to model ebullition fluxes using an ANN. Taking into account that controlling factors are integrators of several parameters, as shown in the previous section via analyses with TSP, change in TSP, and bottom water temperature, the ANN model resulted in much better agreement between calculated and measured ebullition fluxes ( $r^2 = 0.46$ ,  $p < 0.0001$ ; Supplement Fig. S5). Indeed, a step-by-step study with the ANN revealed that the non-linear equation with one input parameter (total change in TSP) gives  $r^2 = 0.26$ . Two input parameters (total change in TSP and TSP) gives  $r^2 = 0.39$ . The addition of bottom temperature leads to the best result of  $r^2 = 0.46$ . The daily time series of the bottom reservoir temperature and atmospheric pressure are shown in Fig. 9a, and the estimated area-weighted modelled ebullitive fluxes together with the measurements at the NT2 Reservoir from January 2009 till August 2013 are shown in Fig. 9b. Over the span of this study, ebullition remained unexpectedly constant, whereas total emissions from hydroelectric reservoirs are known to decrease with time (Abril et al., 2005; Barros et al., 2011) due to the exhaustion of the source of organic matter fuelling the emissions. The modelled ebullitive flux (Fig. 9b) exhibits large seasonal peaks ( $25.9 \pm 9.3 \text{ mmol m}^{-2} \text{ d}^{-1}$ ) at the transition between the CD and WD seasons. The peaks are anticorrelated with the water level variations (Fig. 9b), and occur during the periods when atmospheric pressure is decreasing and water temperature increasing. Due to the high seasonal

variations simulated by ANN, 50 % of the CH<sub>4</sub> emitted by the NT2 Reservoir each year is released within 4 months, even if this period corresponds to the lowest surface of the reservoir. On a yearly basis, ebullition obtained from ANN would represent 60–80 % of the total emission (diffusion and ebullition) at the surface of the NT2 Reservoir. This further supports the idea that the estimate of ebullition from an aquatic ecosystem with large water level variations requires high-frequency measurements over the period of falling water level. This period corresponds to a hot moment of emissions, since the water level as well as its variations and the concomitant temperature variations have a strong impact on ebullition and ultimately on total emissions.

The ANN model allowed us to simulate the ebullition over a four-year period by using a few basic meteorological and limnological input data and a one-year intensive monitoring of CH<sub>4</sub> ebullition. This approach constitutes a powerful gap-filling tool allowing the obtaining of past and future ebullition time series for ecosystems in steady state, like natural wetlands and lakes receiving a constant amount of organic matter from the watershed and under the influence of constant meteorological forcing. However, in the case of a hydroelectric reservoir, this approach must be taken with caution, and can only be applied during short periods of time when the evolution of ebullition is not significant, as is the case for NT2 during our study, or once it reaches its steady state (4–15 years after flooding; Abril et al. 2005; Teodoru et al., 2012).

## 5 Conclusions

Using a set of classical techniques for the discrete measurements of CH<sub>4</sub> diffusion (FC) and ebullition (funnels), and the recently developed EC techniques for the measurement of total CH<sub>4</sub> emissions over large surfaces, we confirmed that the EC system is able to capture continuously and at a 30 min frequency the two main pathways of CH<sub>4</sub> release in inland aquatic ecosystems.

The EC system captured a diurnal bimodal pattern of CH<sub>4</sub> emissions following semi-diurnal variation in the atmospheric pressure. Daily atmospheric air pressure drops during all seasons and whatever the depth of the water column, and triggers CH<sub>4</sub> ebullition, resulting in a first maximum of CH<sub>4</sub> emissions in the middle of the day. At night, a second and moderate peak of CH<sub>4</sub> emissions was recorded due to the combination of a smaller pressure drop and a potential enhancement of the diffusive fluxes because of turbulence generated by heat loss. This might be a common feature in wetlands, where the methanogenesis is active enough to induce a storage of CH<sub>4</sub> in the sediments or flooded soils. This diurnal pattern implies that a precise estimate of CH<sub>4</sub> emissions from aquatic ecosystems requires high-frequency measurements over 24 h in order to capture the daily hot moments of



emissions that could contribute up to 50 % of daily emissions in a few hours.

We have shown that both the concentration of CH<sub>4</sub> in the bubbles reaching the atmosphere and the volume of the bubbles are highly variable. The concentration of CH<sub>4</sub> in bubbles exhibited a high seasonality, suggesting that estimates of ebullition cannot be made by focusing on the volume of bubbles reaching the atmosphere, assuming a predetermined concentration of CH<sub>4</sub> in the bubbles for the whole reservoir and all the seasons.

The CH<sub>4</sub> ebullition mostly depends on the water level and air pressure variations. The use of these linear regressions did not allow a realistic extrapolation of the flux for the entire reservoir (data not shown). This is because of the potential non-linearity of the processes and the complexity of the interactions between the controlling factors. Non-linearity was taken into account using an ANN model with total static pressure, change in total static pressure, and bottom temperature as input parameters. The ANN model was able to explain 46 % of the variation in ebullition CH<sub>4</sub> fluxes, and to perform gap filling for the ebullition fluxes over a four-year period (2009–2013). Our results clearly showed a very high seasonality, with 50 % of the yearly CH<sub>4</sub> ebullition occurring within four months of the WD season, although the surface water area of the reservoir is at its minimum during this period. Overall, ebullition contributed 60–80 % of total emissions at the surface of the reservoir (disregarding downstream emissions). Our results on ebullition in this recently flooded reservoir together with the only other results available in tropical hydroelectric reservoirs (Petit Saut Reservoir, French Guiana; Abril et al., 2005; Galy-Lacaux et al., 1997) during the first year after impoundment suggest that ebullition is a major and overlooked pathway in young tropical or subtropical hydroelectric reservoirs.

**The Supplement related to this article is available online at doi:10.5194/bg-11-4251-2014-supplement.**

*Acknowledgements.* The authors thank everyone who contributed to the NT2 monitoring programme, especially the Nam Theun 2 Power Company (NTPC) and Electricité de France (EDF) for providing financial, technical and logistic support. We are also grateful to the Aquatic Environment Laboratory of the Nam Theun 2 Power Company, whose shareholders are EDF, Lao Holding State Enterprise and Electricity Generating Public Company Limited of Thailand. C. Deshmukh benefited from a PhD grant from EDF. The authors are also grateful to Hydro-Québec for funding and contribution to the logistics of the field trip in March 2011. The authors thank D. Bastviken and an anonymous reviewer for their thorough review of the manuscript.

Edited by: T. J. Battin

## References

- Abril, G., Guérin, F., Richard, S., Delmas, R., Galy-Lacaux, C., Gosse, P., Tremblay, A., Varfalvy, L., Dos Santos, M. A., and Matvienko, B.: Carbon dioxide and methane emissions and the carbon budget of a 10-year old tropical reservoir (Petit Saut, French Guiana), *Global Biogeochem. Cy.*, 19, GB4007, doi:10.1029/2005GB002457, 2005.
- Abril, G., Richard, S., and Guérin, F.: In situ measurements of dissolved gases (CO<sub>2</sub> and CH<sub>4</sub>) in a wide range of concentrations in a tropical reservoir using an equilibrator, *Sci. Total Environ.*, 354, 246–251, 2006.
- Abril, G., Commarieu, M. V., and Guérin, F.: Enhanced methane oxidation in an estuarine turbidity maximum, *Limnol. Oceanogr.*, 52, 470–475, 2007.
- Algar, C. K. and Boudreau, B. P.: Stability of bubbles in a linear elastic medium: Implications for bubble growth in marine sediments, *J. Geophys. Res.-Earth*, 115, F03012, doi:10.1029/2009JF001312, 2010.
- Angel, R. and Conrad, R.: In situ measurement of methane fluxes and analysis of transcribed particulate methane monooxygenase in desert soils. *Environ. Microbiol.*, 11, 2598–2610, 2009.
- Aubinet, M., Grelle, A., Ibrom, A., Rannik, Ü., Moncrieff, J., Foken, T., Kowalski, A. S., Martin, P. H., Berbigier, P., Bernhofer, C., Clement, R., Elbers, J., Granier, A., Grünwald, T., Morgenstern, K., Pilegaard, K., Rebmann, C., Snijders, W., Valentini, R., and Vesala, T.: Estimates of the annual net carbon and water exchange of forests: the EUROFLUX methodology, *Adv. Ecol. Res.*, 30, 113–175, 1999.
- Barros, N., Cole, J. J., Tranvik, L. J., Prairie, Y. T., Bastviken, D., del Giorgio, P., Roland, F., and Huszar, V.: Carbon emission from hydroelectric reservoirs linked to reservoir age and latitude, *Nat. Geosci.*, 4, 593–596, 2011.
- Bastviken, D., Cole, J., Pace, M., and Tranvik, L.: Methane emissions from lakes: dependence of lake characteristics, two regional assessments, and a global estimate, *Global Biogeochem. Cy.*, 18, GB4009, doi:10.1029/2004GB002238, 2004.
- Bastviken, D., Santoro, A. L., Marotta, H., Pinho, L. Q., Calheiros, D. F., Crill, P., and Enrich-Prast, A.: Methane Emissions from Pantanal, South America, during the Low Water Season: Toward More Comprehensive Sampling, *Environ. Sci. Technol.*, 44, 5450–5455, 2010.
- Bastviken, D., Tranvik, L. J., Downing, J. A., Crill, P. M., and Enrich-Prast, A.: Freshwater methane emissions offset the continental carbon sink, *Science*, 331, p. 50, 2011.
- Boles, J. R., Clark, J. F., Leifer, I., and Washburn, L.: Temporal variation in natural methane seep rate due to tides. Coal Oil Point area, California, *J. Geophys. Res.*, 106, 27077–27086, 2001.
- Borges, A. V., Delille, B., Schiettecatte, L.-S., Gazeau, F., Abril, G., and Frankignoulle, M.: Gas transfer velocities of CO<sub>2</sub> in three European estuaries (Randers Fjord, Scheldt and Thames), *Limnol. Oceanogr.*, 49, 1630–1641, 2004.
- Casper, P., Maberly, S. C., Hall, G. H., and Finlay, B. J.: Fluxes of methane and carbon dioxide from a small productive lake to the atmosphere. *Biogeochemistry*, 49, 1–19, 2000.
- Chanton, J. P. and Martens, C. S.: Seasonal variations in the isotopic composition and rate of methane bubble flux from a tidal freshwater estuary, *Global Biogeochem. Cy.*, 2, 289–298, 1988.

- Chanton, J. P., Martens, C. S., and Kelley, C. A.: Gas transport from methane saturated, tidal freshwater and wetland sediments, *Limnol. Oceanogr.*, 34, 807–819, 1989.
- Clement, R.: EdiRe Data Software, v.1.5.0.32; University of Edinburgh, Edinburgh, UK, 1999, available online: <http://www.geos.ed.ac.uk/abs/research/micromet/EdiRe/> (accessed on 12 March 2012).
- Cole, J. J. and Caraco, N. F.: Atmospheric exchange of carbon dioxide in a low-wind oligotrophic lake measured by the addition of SF<sub>6</sub>, *Limnol. Oceanogr.*, 43, 647–656, 1998.
- Cole, J. J., Bade, D. L., Bastviken, D., Pace, M. L., and Van de Bogert, M.: Multiple approaches to estimating air-water gas exchange in small lakes, *Limnol. Oceanogr. Methods*, 8, 285–293, 2010.
- Crawford, J. T., Stanley, E. H., Spawn, S. A., Finlay, J. C., Loken, L. C., and Striegl, R. G.: Ebullitive Methane Emissions from Oxygenated Wetland Streams, *Glob. Change Biol.*, doi:10.1111/gcb.12614, 2014
- Delon, C., Serça, D., Boissard, C., Dupont, R., Dutot, A., Laville, P., De Rosnay, P., and Delmas, R.: Soil NO emissions modelling using artificial neural network, *Tellus B*, 59, 502–513, 2007.
- DelSontro, T., McGinnis, D. F., Sobek, S., Ostrovsky, I., and Wehrli, B.: Extreme Methane Emissions from a Swiss Hydropower Reservoir: Contribution from Bubbling Sediments, *Environ. Sci. Technol.*, 44, 2419–2425, 2010.
- DelSontro, T., Kunz, M. J., Kempter, T., Wüest, A., Wehrli, B., and Senn, D. B.: Spatial heterogeneity of methane ebullition in a large tropical reservoir, *Environ. Sci. Technol.*, 45, 9866–9873, 2011.
- Descloux, S., Chanudet, V., Poilvé, H., and Grégoire, A.: Co-assessment of biomass and soil organic carbon stocks in a future reservoir area located in Southeast Asia, *Environ. Monit. Assess.*, 173, 723–741, 2011.
- Dlugokencky, E. J., Bruhwiler, L., White, J. W. C., Emmons, L. K., Novelli, P. C., Montzka, S. A., Masarie, K. A., Lang, P. M., Crotwell, A. M., Miller, J. B., and Gatti, L. V.: Observational constraints on recent increases in the atmospheric CH<sub>4</sub> burden, *Geophys. Res. Lett.*, 36, L18803, doi:10.1029/2009GL039780, 2009.
- dos Santos, M. A., Rosa, L. P., Sikar, B., Sikar, E., and dos Santos, E. O.: Gross greenhouse gas fluxes from hydro-power reservoir compared to thermo-power plants, *Energ. Policy*, 34, 481–488, 2006.
- Dove, A., Roulet, N., Crill, P., Chanton, J., and Bourbonniere, R.: Methane dynamics of a northern boreal beaver pond, *Ecoscience*, 6, 577–586, 1999.
- Duc, N. T., Crill, P., and Bastviken, D.: Implications of temperature and sediment characteristics on methane formation and oxidation in lake sediments, *Biogeochemistry*, 100, 185–196, 2010.
- Engle, D. and Melack, J. M.: Methane emissions from an Amazon floodplain lake: Enhanced release during episodic mixing and during falling water, *Biogeochemistry*, 51, 71–90, 2000.
- Eugster, W. and Plüss, P.: A fault-tolerant eddy covariance system for measuring CH<sub>4</sub> fluxes. *Agr. Forest Meteorol.*, 150, 841–851, 2010.
- Eugster, W., Kling, G. T., Jonas, J. P., McFadden, A., MacIntyre, S., and Chapin III, F. S.: CO<sub>2</sub> exchange between air and water in an arctic Alaskan and midlatitude Swiss lake: importance of convective mixing, *J. Geophys. Res.*, 108, 4362–4380, 2003.
- Eugster, W., Delsontro, T., and Sobek, S.: Eddy covariance flux measurements confirm extreme CH<sub>4</sub> emissions from a Swiss hydropower reservoir and resolve their short-term variability, *Biogeosciences*, 8, 2815–2831, doi:10.5194/bg-8-2815-2011, 2011.
- Fechner-Levy, E. J. and Hemond, H. F.: Trapped methane volume and potential effects on methane ebullition in a northern peatland, *Limnol. Oceanogr.*, 41, 1375–1383, 1996.
- Foken, T. and Wichura, B.: Tools for quality assessment of surface based flux measurements, *Agric. Forest Meteorol.*, 78, 83–105, 1996.
- Frenzel, P. and Karofeld, E.: CH<sub>4</sub> emission from a hollow-ridge complex in a raised bog, the role of CH<sub>4</sub> production and oxidation, *Biogeochemistry*, 51, 91–112, 2000.
- Frost, T. and Upstill-Goddard, R. C.: Meteorological controls of gas exchange at a small English lake, *Limnol. Oceanogr.*, 47, 1165–1174, 2002.
- Gålfalk, M., Bastviken, D., Fredriksson, S., and Arneborg, L.: Determination of the piston velocity for water-air interfaces using flux chambers, acoustic Doppler velocimetry, and IR imaging of the water surface, *J. Geophys. Res.-Biogeo.*, 118, 770–782, 2013
- Galy-Lacaux, C., Delmas, R., Lambert, C., Dumestre, J. F., Labroue, L., Richard, S., and Gosse, P.: Gaseous emissions and oxygen consumption in hydroelectric dams: A case study in French Guiana, *Global Biogeochem. Cy.*, 11, 471–483, 1997.
- Galy-Lacaux, C., Delmas, R., Kouadio, G., Richard, S., and Gosse, P.: Long term greenhouse gas emission from a hydroelectric reservoir in tropical forest regions, *Global Biogeochem. Cy.*, 13, 503–517, 1999.
- Gardner, M. W. and Dorling, S. R.: Artificial neural networks (The multilayer Perceptron) – a review of applications in the atmospheric sciences, *Atmos. Environ.*, 32, 2627–2636, 1998.
- Gardner, M. W. and Dorling, S. R.: Neural network modelling and prediction of hourly NO<sub>x</sub> and NO<sub>2</sub> concentrations in urban air in London, *Atmos. Environ.*, 33, 709–719, 1999.
- Glaser, P. H., Chanton, J. P., Morin, P., Rosenberry, D. O., Siegel, D. I., Ruud, O., Chasar, L. I., and Reeve, A. S.: Surface deformations as indicators of deep ebullition fluxes in a large northern peatland, *Global Biogeochem. Cy.*, 18, GB1003, doi:10.1029/2003gb002069, 2004.
- Guérin, F. and Abril, G.: Significance of pelagic aerobic methane oxidation in the methane and carbon budget of a tropical reservoir, *J. Geophys. Res.-Biogeo.*, 112, G03006, doi:10.1029/2006JG000393, 2007.
- Guérin, F., Abril, G., Serça, D., Delon, C., Richard, S., Delmas, R., Tremblay, A., and Varfalvy, L.: Gas transfer velocities of CO<sub>2</sub> and CH<sub>4</sub> in a tropical reservoir and its river downstream, *J. Mar. Syst.*, 66, 161–172, 2007.
- Ho, D. T., Bliven, L. F., Wanninkhof, R., and Schlosser, P.: The effect of rain on air–water gas exchange, *Tellus B*, 49, 149–158, 1997.
- Hornik, K., Stinchcombe, M. and White, H.: Multilayer feedforward networks are universal approximators, *Neural Networks*, 2, 359–366, 1989.
- IPCC: Summary for Policymakers, in: *Climate Change 2013: The Physical Science Basis. Contribution of Working Group I to the Fifth Assessment Report of the Intergovernmental Panel on Climate Change*, edited by: Stocker, T. F., Qin, D., Plattner, G.-K., Tignor, M., Allen, S. K., Boschung, J., Nauels, A., Xia, Y., Bex,

- V., and Midgley, P. M., Cambridge University Press, Cambridge, United Kingdom and New York, NY, USA, 2013.
- Jähne, B., Munnich, K. O., Bosinger, R., Dutzi, A., Huber, W., and Libner, P.: On parameters influencing air-water exchange, *J. Geophys. Res.*, 92, 1937–1949, 1987.
- Joyce, J. and Jewell, P. W.: Physical Controls on Methane Ebullition from Reservoirs and Lakes, *Environ. Engineering Geosci.*, 9, 167–178, 2003.
- Keller, M. and Stallard, R. F.: Methane emission by bubbling from Gatun Lake, Panama. *J. Geophys. Res.*, 99, 8307–8319, 1994.
- Kljun, N., Calanca, P., Rotach, M. W., and Schmid, H. P.: A simple parameterization for flux footprint predictions, *Bound-Lay. Meteorol.*, 112, 503–523, 2004.
- Kremer, J. N., Nixon, S. W., Buckley, B., and Roques, P.: Technical note: conditions for using the floating chamber method to estimate air–water gas exchange, *Estuaries*, 26, 985–990, 2003a.
- Kremer, J. N., Reischauer, A., and D’Avanzo, C.: Estuary-specific variation in the air–water gas exchange coefficient for oxygen, *Estuaries*, 26, 829–836, 2003b.
- Krüger, M., Eller, G., Conrad, R., and Frenzel, P.: Seasonal variation in pathways of CH<sub>4</sub> production and in CH<sub>4</sub> oxidation in rice fields determined by stable carbon isotopes and specific inhibitors, *Glob. Change Biol.*, 8, 265–280, 2002.
- Liss, P. and Merlivat, L.: Air-sea exchange rates: introduction and synthesis, in: *The role of air-sea exchanges in geochemical cycling*, edited by: Buat-Meinard, P., Reidel, Dordrecht, 113–127, 1986.
- Liss, P. S. and Slater, P. G.: Flux of gases across the air–sea interface, *Nature*, 233, 327–329, 1974.
- MacIntyre, S., Romero, J. R., and Kling, G. W.: Spatial-temporal variability in mixed layer deepening and lateral advection in an embayment of Lake Victoria, East Africa, *Limnol. Oceanogr.*, 47, 656–671, 2002.
- MacIntyre, S., Jonsson, A., Jansson, M., Aberg, J., Turney, D. E., and Miller, S. D.: Buoyancy flux, turbulence, and the gas transfer coefficient in a stratified lake, *Geophys. Res. Lett.*, 37, L24604, doi:10.1029/2010GL044164, 2010.
- Mahrt, L., Sun, J., Blumen, W., Delany, T., and Oncley, S.: Nocturnal boundary-layer regimes, *Bound-Lay. Meteorol.*, 88, 255–278, 1998.
- Martens, C. S. and Klump, J. V.: Biogeochemical cycling in an organic-rich coastal marine basin, 4. An organic carbon budget for sediments dominated by sulfate reduction and methanogenesis, *Geochim. Cosmochim. Ac.*, 48, 1987–2004, 1980.
- Matthews, C. J. D., St-Louis, V. L., and Hesslein, R. H.: Comparison of three techniques used to measure diffusive gas exchange from sheltered aquatic surfaces, *Environ. Sci. Technol.*, 37, 772–780, 2003.
- Mattson, M. D. and Likens, G. E.: Air pressure and methane fluxes, *Nature*, 347, 718–719, 1990.
- McDermitt, D., Burba, G., Xu, L., Anderson, T., Komissarov, A., Riensch, B., Schedlbauer, J., Starr, G., Zona, D., Oechel, W., Oberbauer, S., and Hastings, S.: A new low-power, open-path instrument for measuring methane flux by eddy covariance, *Appl. Phys. B*, 102, 391–405, 2011.
- McGinnis, D. F., Greinert, J., Artemov, Y., Beaubien, S. E., and Wüest, A.: The fate of rising methane bubbles in stratified waters: how much methane reaches the atmosphere?, *J. Geophys. Res.*, 111, C09007, doi:10.1029/2005JC003183, 2006.
- Morrissey, L. A. and Livingston, G. P.: Methane emissions from Alaska Arctic tundra: An assessment of local spatial variability, *J. Geophys. Res.*, 97, 16661–16670, 1992.
- NTPC (Nam Theun 2 Power Company): Environmental Assessment and Management Plan – Nam Theun 2 Hydroelectric Project, Nam Theun 2 Power Company, Vientiane, Internal report, 212 pp., 2005.
- Ostrovsky, I., McGinnis, D. F., Lapidus, L., and Eckert, W.: Quantifying gas ebullition with echosounder: the role of methane transport by bubbles in a medium-sized lake, *Limnol. Oceanogr.-Meth.*, 6, 105–118, 2008.
- Rothfuss, F. and Conrad, R.: Vertical profiles of CH<sub>4</sub> concentrations, dissolved substrates and processes involved in CH<sub>4</sub> production in a flooded Italian rice field, *Biogeochemistry*, 18, 137–152, 1992.
- Sahlée, E., Rutgersson, A., Podgrajsek, E., and Bergström, H.: Influence from surrounding land on the turbulence measurements above a lake, *Bound-Lay. Meteorol.*, 150, 235–258, 2014.
- Schubert, C. J., Diem, T., and Eugster, W.: Methane emissions from a small wind shielded lake determined by eddy covariance, flux chambers, anchored funnels, and boundary model calculations: a comparison, *Environ. Sci. Technol.*, 46, 4515–4522, 2012.
- Smith, L. K., Lewis, W. M., Chanton, J. P., Cronin, G., and Hamilton, S. K.: Methane emissions from the Orinoco River floodplain, Venezuela, *Biogeochemistry*, 51, 113–140, 2000.
- Teodoru, C. R., Bastien, J., Bonneville, M. C., del Giorgio, P. A., Demarty, M., Garneau, M., Hélie, J. F., Pelletier, L., Prairie, Y. T., Roulet, N. T., Strachan, I. B., and Tremblay, A.: The net carbon footprint of a newly-created boreal hydroelectric reservoir, *Global Biogeochem. Cy.*, 26, GB2016, doi:10.1029/2011, 2012.
- Tokida, T., Miyazaki, T., and Mizoguchi, M.: Ebullition of methane from peat with falling atmospheric pressure, *Geophys. Res. Lett.*, 32, L13823, doi:10.1029/2005GL022949, 2005.
- Tyler, S. C., Bilek, R. S., Sass, R. L., and Fischer, F. M.: Methane oxidation and pathways of production in a Texas paddy field deduced from measurements of flux,  $\delta^{13}\text{C}$ , and  $\delta D$  of CH<sub>4</sub>, *Global Biogeochem. Cy.*, 11, 323–348, 10.1029/97gb01624, 1997.
- Vachon, D., Prairie, Y. T., and Cole, J. J.: The relationship between near-surface turbulence and gas transfer velocity in freshwater systems and its implications for floating chamber measurements of gas exchange, *Limnol. Oceanogr.*, 55, 1723–1732, 2010.
- Vapnik, V. N.: *The nature of statistical learning theory*, Springer, 1995.
- Varadharajan, C. and Hemond, H. F.: Time-series analysis of high-resolution ebullition fluxes from a stratified, freshwater lake, *J. Geophys. Res.-Biogeo.*, 117, G02004, doi:10.1029/2011JG001866, 2012.
- Vickers, D. and Mahrt, L.: Quality control and flux sampling problems for tower and aircraft data, *J. Atmos. Ocean. Tech.*, 14, 512–526, 1997.
- Walter, K. M., Chanton, J. P., Chapin III, F. S., Schuur, E. A. G., and Zimov, S. A.: Methane production and bubble emissions from arctic lakes: Isotopic implications for source pathways and ages, *J. Geophys. Res.*, 113, G00A08, doi:10.1029/2007JG000569, 2008.
- Wanninkhof, R.: Relationship between gas exchange and wind speed over the ocean. *J. Geophys. Res.*, 97, 7373–7382, 1992.

Wik, M., Crill, P. M., Varner, R. K., and Bastviken, D.: Multiyear measurements of ebullitive methane flux from three subarctic lakes, *J. Geophys. Res.-Biogeo.*, 118, 1307–1321, 2013.

WMO: Guide to Meteorological Instruments and Methods of Observation WMO-No, 8 pp., 2008.

Yamamoto, S., Alcauskas, J. B., and Crozier, T. E.: Solubility of methane in distilled water and seawater, *J. Chem. Eng. Data*, 21, 78–80, 1976.